Diffraction of waves by arbitrary crack configurations in ice sheets

R. Porter

School of Mathematics, University of Bristol, Bristol, BS8 1TW, UK.

July 31, 2006

Abstract

The interaction of plane waves propagating within a uniform ice sheet above sea water with narrow cracks of arbitrary shape is considered in this paper. The motion of the fluid is described by linearised theory and the ice sheet is modelled as as thin elastic plate. A complete description of the solution is shown to be expressible in terms of pairs of functions related to the jumps in the gradient across, and elevation of, the narrow cracks in the ice sheet. These functions are determined by the solution of a set of coupled integro-differential equations which can, in principle, be solved numerically for any crack shape. However, attention focuses on the case of multiple straight-line cracks, of arbitrary orientation, for which further simplifying analytic progress can be made before computations are performed. Results presented showing diffracted wave patterns, stress intensity factors at the ends of cracks and the elevation of the ice sheet along the cracks.

The problem of determining flexural wave diffraction by narrow cracks in a thin elastic plate with no fluid loading is a much simpler limiting case of the present problem.

1 Introduction

This paper is a continuation of a series of papers involving the current author on the subject of wave scattering by cracks in thin ice sheets over water. The problems considered are intended to assist understanding of the wave scattering processes that occur in the large regions of the Arctic and Antartic seas known as the marginal ice-zone, situated between the open oceans and the shore-fast sea ice, where there is a dense packing of large ice sheets which continually crack and reform under the action of waves and currents. The wave energy originates from the ocean waves and propagtes far into the marginal ice-zone in the form of flexural-gravity waves supported at the interface between the atmosphere, the ice sheet and the underlying fluid. Experimental evidence (see Squire *et al* (1995), for example) suggest that classical thin plate theory is a good model for ice sheets although more complicated models have also been used (see Balmforth & Craster (1999), for example). Models of wave scattering by cracks can be useful in determining if, and where, further breakup of ice is likely to occur, but also as a remote sensing tool for determining variations in ice sheet size and thickness (see Williams (2005) or Vaughan & Squire (2006)). Another application area is in the offshore industry where cracks may occur (or be part of the design) in so-called very

large floating structures such as those being proposed and tested for use as offshore runways in Japan where the same governing equations are employed.

Previous work in this subject area includes wave scattering by a single infinitely long crack between two semi-infinite ice sheets by Evans & Porter (2003) who took advantage of the symmetry of the geometry to decompose the problem into two separate problems for the symmetric and antisymmetric components of the solution. Reflection and transmission coefficients were computed for a range of parameters and it was also shown that edge waves could propagate along the crack, without radiating energy away from the crack. The work of Evans & Porter (2003) was very closely related to work by researchers in New Zealand including Barrett & Squire (1999), Squire & Dixon (2001) and Williams & Squire (2002). The work on the single crack was generalised to multiple infinitely long parallel cracks in Porter & Evans (2006a) who introduced the use of 'source functions' as a simple and elegant method for representing the solution. Thus, in the problem considered in Porter & Evans (2006a) the entire scattering process was shown to be represented by an incident wave plus a pair of generalised line sources placed along each of the cracks in the configuration. Outgoing waves are generated by the source functions by imposing certain jump conditions in the function and its derivatives at the source. Other work on multiple cracks includes that of Williams & Squire (2004) using Green functions.

Following that, the problem of *finite* straight parallel cracks was considered in Porter & Evans (2006b). In this problem, advantage was taken of the fact that Fourier Transforms in the direction of the cracks reduced the problem to the quasi-two dimensional problem of Porter & Evans (2006a). That work also relied heavily on the work of Andronov & Belinskii (1995) who had considered scattering by a single finite length crack in a thin elastic plate *in vacuo*. Scattering by semi-infinite cracks in unloaded elastic plates has been undertaken by Norris & Wang (1994).

The present piece of work represents a substantial departure from that which has gone before. Here, we formulate the solution to the problem of scattering by a general connfiguration of multiple cracks of arbitrary shape. However, the present work is a natural extension of previous papers by the author in that the solution can be represented by a superposition of an incident wave from infinity plus a distribution of a pair of generalised point source functions, w_1 and w_2 of source strength $P_i(s)$ and $Q_i(s)$, $s \in \mathcal{C}_i$, along each of the N cracks, $\mathcal{C}_i$, $i = 1, \ldots, N$.

By applying the two boundary conditions along each of the N cracks results in $2N$ coupled integro-differential equations $2N$ unknown functions $P_i(s)$ and $Q_i(s)$, $i = 1, \ldots, N$.

Despite the apparent elegance of the solution method described above, there are many technical difficulties associated with trying to compute solutions to the integro-differential equations (for a general overview see Martin (2006, §5.3.1) where they are called hypersingular integral equations). The first, also encountered in Porter & Evans (2006b), is identifying and then treating the most singular part of the source functions as they would otherwise give rise to divergent integrals (being two and four derivatives of a logarithm). The second is that the pair of generalised source functions are found to be complicated second and third-order differential operators associated with the boundary conditions on the cracks applied to a relatively straightforward canonical Green function. The integro-differential equations that determine the functions $P_i(s)$ and $Q_i(s)$ involve a second application of the same differential operators implying that the kernels of certain integral operators are compound fourth to sixth-order differential operators defined in coordinates local to the crack of varying shape. Thus, whilst the problem is easy to formulate, the implementation of a numerical scheme to

find solutions appears to be a non-trivial task.

In this paper, we have removed some of this difficulty by only considering results for cracks which are straight, but consider multiple cracks which can be oriented at arbitrary angles to one another, a case not possible using the transform approach of Porter & Evans (2006b). In fact it is shown that the system of equations derived and computed in Porter & Evans (2006b) is recovered from current method if all cracks are parallel.

The mathematical formulation of each part of this paper is quite treacherous and much of the lengthy algebraic detail has had to be suppressed. In the next section, we concentrate on the case of a single curvilinear crack and present the equations governing the motion of the ice sheet and the fluid as well as the various boundary conditions that must be imposed including those along the cracks, at the ends of the cracks and at infinity. In section 3, a set of equations and conditions are stated which define the pair of source functions which are to be distributed along each crack. An integral representation for the solution is then presented in terms of these source functions. The source functions are then derived in closed form by taking double Fourier transforms in the surface of the elastic plate and using the various definitions of the source functions to show that they are related to a fundamental Green function for an elastic plate over water, described in an obscure report by Fox & Chung (1998), but rederived for completeness in the Appendix of the present paper. In the last parts of section 3 the coupled integro-differential equations for the undetermined functions $P(s)$ and $Q(s)$ are presented, by application of the two boundary conditions on the crack and we give a detailed description of how to treat the potentially singular part of the integral equations. In particular, we suggest that straight-line cracks appear to offer the only way of proceeding analytically from this point onwards. Thereafter, the paper considers multiple straight-line cracks at arbitrary angles to one another. Thus in section 4 the integro-differential equations are reduced to infinite systems of equations by expanding the unknown functions in an infinite series of judiciously chosen functions which include the correct weighting at the ends of the cracks The integro-differential equations are thus converted into an infinite algebraic system of equations by the Rayleigh-Ritz method (equivalent to Galerkin's method) and efficient numerical solutions are found by truncation to a small finite system. An integral representation of the Hankel function and a re-alignment of the coordinate system to that of each crack in turn is the key to the success of the method which results in a system of equations in which the matrix elements just involve the computation of relatively straightforward and highly convergent infinite integrals.

In section 5, we show how to recover, from the solution to the system of equations, the elevation of the elastic plate, the far-field diffracted wave amplitudes and the stress intensity factors at the ends of the cracks. Finally, in section 6, numerical results are presented and we summarise the paper in section 7.

2 Governing equations

Cartesian coordinates, (x, y, z) are defined with z directed vertically upwards. When at rest, the lower surface of an ice sheet of small thickness d occupies the plane $z = 0$ and the water is bounded below by $z = -h$. A plane wave is incident from infinity and propagates along the ice sheet at an angle φ with respect to the positive x-axis.

For simplicity, we initially concentrate on the case where there is just a single crack. The subsequent extension to multiple cracks is relatively straightforward. Thus the incident

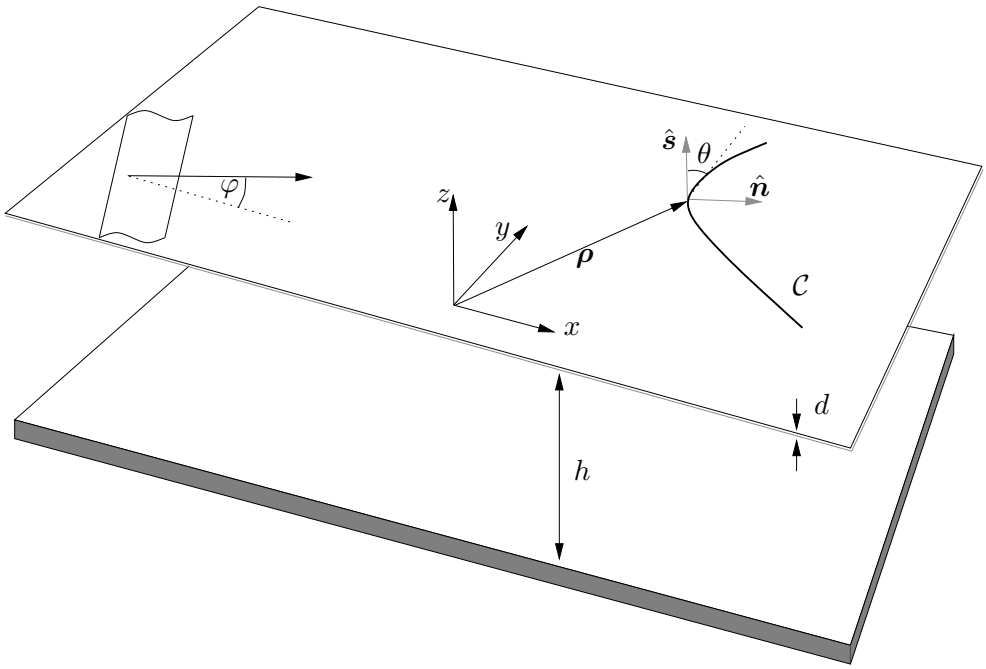

Figure 1: Geometrical description of the ice sheet containing a crack over water

wave is diffracted by a narrow crack in the ice sheet represented by the two-dimensional line $\mathcal{C}$, and parametrised by the arclength along the curve, s where $-L < s < L$, so that $(x(s), y(s)) \in \mathcal{C}$. The length of the crack is thus $2L$.

The ice sheet is modelled as a thin elastic plate using Kirchhoff theory and at the edges of the cracks the bending moment and shearing stress must vanish (see Timoshenko & Woinowsky-Krieger (1959), for example)

2.1 Equations governing the motion of the fluid and the ice sheet

Under the assumptions of linearised theory, that the fluid is incompressible and inviscid and that the motion is irrotational and of small amplitude, we may define a velocity potential, $\Phi(\boldsymbol{r}, t)$, where $\boldsymbol{r} = (x, y, z)$ in the fluid region $\mathcal{W} = \{(x, y) \in \mathbb{R}^2, -h < z < 0\}$ where $\mathbb{R}^2 = \{-\infty < x, y < \infty\}$, and assuming a time harmonic dependence of angular frequency ω we write

$$\Phi(\boldsymbol{r}, t) = \Re\{-\mathrm{i}\omega\phi(\boldsymbol{r})\mathrm{e}^{-i\omega t}\}. \tag{2.1}$$

The elevation of the fluid surface and hence the deflection of the ice sheet from equilibrium is defined by $\Re\{\eta(\boldsymbol{\rho})\mathrm{e}^{-\mathrm{i}\omega t}\}$ where $\boldsymbol{\rho} = (x, y)$ and

$$\eta(\boldsymbol{\rho}) = \left.\frac{\partial\phi}{\partial z}\right|_{z=0}, \qquad \boldsymbol{\rho} \in \mathbb{R}^2 \backslash \mathcal{C}. \tag{2.2}$$

It follows that $\phi(\boldsymbol{r})$ satisfies

$$\Delta\phi = 0, \qquad \boldsymbol{r} \in \mathcal{W} \tag{2.3}$$

where Δ is used to denote the three-dimensional Laplacian operator, $\Delta = \nabla^2 + \partial^2/\partial z^2$, where $\nabla = (\partial/\partial x, \partial/\partial y)$,

$$\frac{\partial\phi}{\partial z} = 0, \quad z = -h, \boldsymbol{\rho} \in \mathbb{R}^2, \tag{2.4}$$

and

$$\big(\mathcal{L}\phi\big)(\boldsymbol{\rho}) \equiv \big(D\nabla^4 + 1 - \delta\big)\,\eta - \kappa\phi|_{z=0} = 0, \qquad \boldsymbol{\rho} \in \mathbb{R}^2 \backslash \mathcal{C}. \tag{2.5}$$

In the above, $\kappa = \omega^2/g$ where g is gravitational acceleration and D is defined by $D = Ed^3/(12\rho_w g(1-\nu^2))$ where E is the Young's Modulus, ν is Poisson's ratio, d is the thickness of the ice sheet and ρ_w is the density of the fluid. Also $\delta = (\rho_i/\rho_w)\kappa d$ where ρ_i is the density of ice.

Worthy of note is the non-dimensionalisation described in detail in Williams (2005) (also see Williams & Squire (2004)) in which characteristic lengthscales and timescales are defined which reduce the number of parameters appearing in the governing equations (excluding any parametrisation of the crack) to just two. This can be useful in analysing the results to certain simpler problems, although it proves to be of no benefit here.

2.2 Boundary conditions on the cracks

Before considering the boundary conditions at the edges of the cracks, we are required to consider certain features associated with the curve $\mathcal{C}$. Thus the unit vectors tangential to and normal to $\mathcal{C}$, as a function of arclength s are defined (respectively) by

$$\left.\begin{aligned} \hat{\boldsymbol{s}}(s) &= (x'(s), y'(s))/\mu(s) \\ \hat{\boldsymbol{n}}(s) &= (y'(s), -x'(s))/\mu(s) \end{aligned}\right\} \qquad \text{where } \mu(s) = \sqrt{x'(s)^2 + y'(s)^2} \tag{2.6}$$

and primes deonte differentiation with respect to the argument.

In particular, we denote the angle between the positive x-direction and the direction of $\hat{\boldsymbol{n}}$ by $\theta(s)$, so that $\theta'(s)$ is simply the curvature of $\mathcal{C}$. Then $\hat{\boldsymbol{n}} = \cos\theta\boldsymbol{i} + \sin\theta\boldsymbol{j}$ and $\hat{\boldsymbol{s}} = -\sin\theta\boldsymbol{i} + \cos\theta\boldsymbol{j}$ and we have

$$\hat{\boldsymbol{n}}.\nabla \equiv \frac{\partial}{\partial n} = \cos\theta\frac{\partial}{\partial x} + \sin\theta\frac{\partial}{\partial y}, \qquad \hat{\boldsymbol{s}}.\nabla \equiv \frac{\partial}{\partial s} = -\sin\theta\frac{\partial}{\partial x} + \cos\theta\frac{\partial}{\partial y},$$

and it follows that the two-dimensional Laplacian can be written

$$\nabla^2 = \frac{\partial^2}{\partial n^2} + \frac{\partial^2}{\partial s^2} + \theta'(s)\frac{\partial}{\partial n} \tag{2.7}$$

with the auxiliary equation

$$\frac{\partial}{\partial n}\frac{\partial}{\partial s} - \frac{\partial}{\partial s}\frac{\partial}{\partial n} + \theta'(s)\frac{\partial}{\partial s} = 0 \tag{2.8}$$

which demonstrates that $\partial/\partial n$ and $\partial/\partial s$ do not, in general, commute in these generalised coordinates.

We can now define conditions that apply along the free edges $\mathcal{C}_-$ and $\mathcal{C}_+$ (defined such that $\hat{\boldsymbol{n}}$ points in the direction from $\mathcal{C}_-$ to $\mathcal{C}_+$) either side of the curve $\mathcal{C}$. First, the bending moment vanishes at the edges of the crack, and this is expressed by the operator equation

$$\big(\mathcal{B}\eta\big)(\boldsymbol{\rho}) \equiv \left(\nabla^2 - \nu_1\left(\frac{\partial^2}{\partial s^2} + \theta'(s)\frac{\partial}{\partial n}\right)\right)\eta \to 0, \qquad \text{as } \boldsymbol{\rho} \to \mathcal{C}_\pm \tag{2.9}$$

and secondly the shearing stress is zero along the edges, which is expressed as

$$\big(\mathcal{S}\eta\big)(\boldsymbol{\rho}) \equiv \left(\frac{\partial}{\partial n}\nabla^2 + \nu_1\frac{\partial}{\partial s}\left(\frac{\partial}{\partial s}\frac{\partial}{\partial n} - \theta'(s)\frac{\partial}{\partial s}\right)\right)\eta \to 0, \qquad \text{as } \boldsymbol{\rho} \to \mathcal{C}_\pm \tag{2.10}$$

where $\nu_1 = 1 - \nu$. Note that the definitions of the operators in (2.9) and (2.10), which strictly are defined only on $\mathcal{C}$ itself, have been extended to points away from $\mathcal{C}$. Note also that the limits in (2.9) and (2.10) and hereafter, expressed as $\boldsymbol{\rho} \to \mathcal{C}_\pm$ are to be intepreted as meaning $(\boldsymbol{\rho} - (x(s), y(s))).\hat{\boldsymbol{s}} = 0$ with $(\boldsymbol{\rho} - (x(s), y(s))).\hat{\boldsymbol{n}} \to 0^\pm$. That is, that the point approaches the curve in the direction normal to the curve.

As a consequence of (2.9) and (2.10),

$$\big[\big(\mathcal{B}\eta\big)(\boldsymbol{\rho})\big] = \big[\big(\mathcal{S}\eta\big)(\boldsymbol{\rho})\big] = 0, \tag{2.11}$$

where here we have used, and will continue to use, the square bracket notation to indicate the jump in the enclosed quantities across $\mathcal{C}$ in a direction normal to $\mathcal{C}$ from $\mathcal{C}_+$ to $\mathcal{C}_-$. That is, for a general function $u(\boldsymbol{\rho})$,

$$\big[u(\boldsymbol{\rho})\big] \equiv \lim_{\boldsymbol{\rho}\to\mathcal{C}_+}\{u(\boldsymbol{\rho})\} - \lim_{\boldsymbol{\rho}\to\mathcal{C}_-}\{u(\boldsymbol{\rho})\}. \tag{2.12}$$

2.3 Separation solutions and the radiation condition

To complete the formulation of the problem we need to impose a radiation condition on the diffracted wave field and before doing this we first consider separable solutions of (2.3) for an ice sheet which contains no cracks. These are given by

$$\exp\{\mathrm{i}\boldsymbol{k}_n.\boldsymbol{\rho}\}Y_n(z), \qquad \text{for } n = -2, -1, 0, 1, \ldots \tag{2.13}$$

where $\boldsymbol{k}_n = k_n(\cos w_n, \sin w_n)$ for some arbitrary angle $w_n \in [0, 2\pi)$. and where

$$Y_n(z) = \cosh k_n(z + h) \tag{2.14}$$

are depth eigenfunctions and k_n are the roots of the dispersion relation

$$K(k_n) \equiv (Dk_n^4 + 1 - \delta)k_n \sinh k_n h - \kappa \cosh k_n h = 0. \tag{2.15}$$

In (2.13) and (2.14), k_0 is the positive real root of (2.15). There are an infinite sequence of pure imaginary roots of (2.15) and k_n, $n = 1, 2, \ldots$ are defined as those with positive imaginary parts arranged such that $|k_n| < |k_{n+1}|$. In addition, there are four (generally) complex roots of (2.15) which are defined as $\pm p \pm \mathrm{i}q$, $p, q > 0$ and k_{-1} is defined as $p + \mathrm{i}q$, whilst $k_{-2} = -p + \mathrm{i}q$. For certain (somewhat extreme) values of physical parameters, the complex roots can move onto the imaginary axis. Details of the location and nature of the roots is discussed in detail in Williams (2005). Also see Squire *et al* (1995).

The depth eigenfunctions satisfy a generalised orthogonality relation

$$\kappa \int_{-h}^{0} Y_n(z)Y_m(z)dz + D(k_m^2 + k_n^2)Y_m'(0)Y_n'(0) = C_n\delta_{nm} \tag{2.16}$$

which can be established by integrating by parts (see, for example, Lawrie & Abrahams 2002) where

$$C_n = \tfrac{1}{2}\{\kappa h + (5Dk_n^4 + 1 - \delta)[Y_n'(0)/k_n]^2\} \tag{2.17}$$

and δ_{mn} is the Kronecker Delta.

An incident wave from infinity, propagating at an angle of φ with respect to the positive x-axis, is described by the potential

$$\phi_0(\boldsymbol{r}) = \mathrm{e}^{\mathrm{i}k_0(x\cos\varphi + y\sin\varphi)}Y_0(z) \tag{2.18}$$

with corresponding surface elevation given by

$$\eta_0(\boldsymbol{\rho}) = \mathrm{e}^{\mathrm{i}k_0(x\cos\varphi + y\sin\varphi)} Y_0'(0). \tag{2.19}$$

For an incident wave of (complex) amplitude A a scaling of $A/Y_0'(0)$ should be applied to both η and ϕ throughout. Then the radiation conditions to be satisfied by both $u = \phi_d = \phi - \phi_0$ and $u = \eta_d = \eta - \eta_0$ is

$$\sqrt{\rho}\left(\frac{\partial}{\partial\rho} - \mathrm{i}k_0\right) u \to 0, \qquad \text{as } \rho = |\boldsymbol{\rho}| = \sqrt{x^2+y^2} \to \infty, \tag{2.20}$$

holding throughout $-h < z < 0$ in the former definition.

2.4 Properties associated with cracks

In the course of the analysis, it will be shown that the quantities

$$Q(s) = [\eta], \qquad P(s) = \left[\frac{\partial\eta}{\partial n}\right], \qquad -L < s < L \tag{2.21}$$

where $2L$ is the length of the crack, play a significant role. Thus, $Q(s)$ and $P(s)$ represent the jumps, across the crack, in the elevation and the component of gradient normal to the crack (respectively).

Certain conditions also apply at the two ends of the crack. First

$$[\eta] \sim (L^2-s^2)^{3/2}, \quad \left[\frac{\partial\eta}{\partial n}\right] \sim (L^2-s^2)^{1/2}, \quad \left[\frac{\partial\eta}{\partial s}\right] \sim (L^2-s^2)^{1/2}, \qquad \text{as } s \to -L^+, L^-. \tag{2.22}$$

The above expressions are Meixner conditions (see Andronov & Belinskii (1995), for example) which can be derived from a local analysis of the plate deflection in the neighbourhood of a crack tip.

Also, the requirement that no concentrated forces exist at the ends of the crack, implies

$$\left[\frac{\partial^2\eta}{\partial n\partial s}\right] = \left[\left(\frac{\partial^2}{\partial s\partial n} - \theta'(s)\frac{\partial}{\partial s}\right)\eta\right] = 0, \qquad \text{as } s \to -L^+, L^-, \tag{2.23}$$

conditions which will be of use later.

3 Formulation of integral equations

Integral equations can be derived in one of two ways. The first comes about from a direct application of Green's Identity to a source in the fluid with the function ϕ and follows using much of the analysis from equation (3.16) onwards. The second approach, presented here, is arguably more natural and allows the general solution to be presented rather than derived, once a pair of 'source' functions have been appropriately defined. The hard work is relegated to the derivation of expressions for these source functions.

3.1 Definition of a pair of source functions

The first step is to construct point 'source' functions which act along at points $\boldsymbol{\rho}_0 \in \mathcal{C}$ along the curve, where we may also write $\boldsymbol{\rho}_0 \equiv (x_0, y_0) \equiv (x(s_0), y(s_0))$, $-L < s_0 < L$. These functions will be then used to formulate a solution to the problem defined in the previous section. Thus, we seek a pair of functions $\psi_i(\boldsymbol{r}; \boldsymbol{\rho}_0)$, $i = 1, 2$ satisfying the following conditions,

$$\Delta\psi_i = 0, \qquad \boldsymbol{r} \in \mathcal{W} \tag{3.1}$$

with

$$\frac{\partial\psi_i}{\partial z} = 0, \qquad z = -h, \ \boldsymbol{\rho} \in \mathbb{R}^2 \tag{3.2}$$

and

$$(\mathcal{L}\psi_i)(\boldsymbol{\rho}; \boldsymbol{\rho}_0) \equiv \left(D\nabla^4 + 1 - \delta\right) w_i - \kappa\psi_i|_{z=0} = 0, \qquad \text{for } \boldsymbol{\rho} \neq \boldsymbol{\rho}_0 \tag{3.3}$$

where

$$w_i(\boldsymbol{\rho}; \boldsymbol{\rho}_0) = \left.\frac{\partial\psi_i}{\partial z}\right|_{z=0} \tag{3.4}$$

for $i = 1, 2$, is the surface elevation associated with the functions ψ_i. We require that ψ_i and hence w_i represent outgoing waves as $|\boldsymbol{\rho}| \to \infty$, and hence satisfy (2.20). Finally we impose the following jump conditions as defined by (2.12)

$$\left[w_1\right] = 0, \qquad \left[\frac{\partial w_1}{\partial n}\right] = \delta(s - s_0), \qquad -L < s, s_0 < L \tag{3.5}$$

and

$$\left[w_2\right] = \delta(s - s_0), \qquad \left[\frac{\partial w_2}{\partial n}\right] = 0, \qquad -L < s, s_0 < L \tag{3.6}$$

where $\delta(x)$ is the Dirac delta function which provide the only source of forcing for ψ_1 and ψ_2. These are supplemented by jump conditions associated with the free edge operators defined by (2.9) and (2.10),

$$\left[\left(\mathcal{B}w_i\right)(\boldsymbol{\rho}; \boldsymbol{\rho}_0)\right] = \left[\left(\mathcal{S}w_i\right)(\boldsymbol{\rho}; \boldsymbol{\rho}_0)\right] = 0, \qquad -L < s, s_0 < L \tag{3.7}$$

for $i = 1, 2$. The source functions will be derived in section 3.3.

3.2 An integral represention for the solution

Assuming the existence of the functions ψ_i the general solution, in terms of undetermined functions $P(s_0)$ and $Q(s_0)$, may be written as

$$\phi(\boldsymbol{r}) = \phi_0(\boldsymbol{r}) + \int_{-L}^{L} \left\{P(s_0)\psi_1(\boldsymbol{r}; \boldsymbol{\rho}_0) + Q(s_0)\psi_2(\boldsymbol{r}; \boldsymbol{\rho}_0)\right\} \mathrm{d}s_0 \tag{3.8}$$

with corresponding surface elevation clearly following as

$$\eta(\boldsymbol{\rho}) = \eta_0(\boldsymbol{\rho}) + \int_{-L}^{L} \left\{P(s_0)w_1(\boldsymbol{\rho}; \boldsymbol{\rho}_0) + Q(s_0)w_2(\boldsymbol{\rho}; \boldsymbol{\rho}_0)\right\} \mathrm{d}s_0. \tag{3.9}$$

The justification for this form of the solution follows since (2.4), (2.5) and (2.6) are clearly satisfied. Also, from (3.7) since it can be seen from (3.9) that $\eta(\boldsymbol{\rho})$ satisfies (2.11) and the

radiation condition (2.20). Finally, by taking jumps in η and $\partial\eta/\partial n$ from (3.9) and using the imposed conditions in (3.6) on w_1 and w_2 justifies the definition of P and Q in (2.21).

The remaining conditions that are *not* satisfied by (3.9) are the edge conditions (2.9) and (2.10), although the satisfication of (2.11) by (3.9) implies that these only need to be applied from one side of $\mathcal{C}$.

It is helpful to interpret the solution presented in (3.8), (3.9) as a distribution of two different types of "sources" along the crack, each having an associated "source strength", being the two functions P and Q. Indeed, this is a rather natural viewpoint to take, as the only source of scattering is the crack itself whilst the fact that two sources are needed can either be attributed to the order of the differential operator defining the motion of the ice sheet, or (in fact, equivalently) that two boundary conditions are required on the crack. Furthermore, it is a natural generalisation of similar solution methods developed for more specific problems (see Porter & Evans (2006a,b)).

3.3 Calculation of the source functions

In order to construct the functions ψ_i, we take Fourier transforms in x and y, defining

$$\overline{\psi}_i(\alpha,\beta,z;\boldsymbol{\rho}_0)=\int_{-\infty}^{\infty}\int_{-\infty}^{\infty}\psi_i(\boldsymbol{r};\boldsymbol{\rho}_0)\mathrm{e}^{\mathrm{i}(\alpha x+\beta y)}\,\mathrm{d}x\mathrm{d}y. \tag{3.10}$$

It is straightforward to show from (3.1) and (3.2) that

$$\overline{\psi}_i(\alpha,\beta,z;\boldsymbol{\rho}_0)=A_i(\alpha,\beta)\cosh k(z+h) \tag{3.11}$$

for $i=1,2$ where $k^2=\alpha^2+\beta^2$ and $A_i(\alpha,\beta)$ is to be determined from the transform of the surface condition (3.3),

$$0=\int_{-\infty}^{\infty}\int_{-\infty}^{\infty}\big(\mathcal{L}\psi_i\big)(x,y;\boldsymbol{\rho}_0)\mathrm{e}^{\mathrm{i}(\alpha x+\beta y)}\,\mathrm{d}x\mathrm{d}y=(Dk^4+1-\delta)\overline{w}_i-\kappa\overline{\psi}_i+DI_i \tag{3.12}$$

where

$$\overline{w}_i(\alpha,\beta;\boldsymbol{\rho}_0)=\left.\frac{\partial\overline{\psi}_i}{\partial z}\right|_{z=0} \tag{3.13}$$

and

$$I_i=I_i(\alpha,\beta;\boldsymbol{\rho}_0)=\int_{-\infty}^{\infty}\int_{-\infty}^{\infty}G(\nabla^4 w_i)\,\mathrm{d}x\mathrm{d}y-k^4\overline{w}_i \tag{3.14}$$

where we have introduced, for brevity,

$$G=G(\boldsymbol{\rho};\alpha,\beta)=\mathrm{e}^{\mathrm{i}(\alpha x+\beta y)}. \tag{3.15}$$

The result (3.12) follows since Fourier transforms of w_i and ψ_i can immediately be taken (integrals of functions with at most finite jump discontinuities are well defined), but not Fourier transforms of higher derivatives of w_i which require more care.

In order to evaluate the integral in (3.14), we use Greens Identity applied to the biharmonic operator to write

$$\begin{aligned} I_i &= \int_{-\infty}^{\infty}\int_{-\infty}^{\infty}\big(G(\nabla^4 w_i)-w_i(\nabla^4 G)\big)\,\mathrm{d}x\mathrm{d}y \\ &= \int_{C_-\cup C_+}\left(G\frac{\partial}{\partial n}(\nabla^2 w_i)-w_i\frac{\partial}{\partial n}(\nabla^2 G)-(\nabla^2 w_i)\frac{\partial G}{\partial n}+(\nabla^2 G)\frac{\partial w_i}{\partial n}\right)\mathrm{d}s \end{aligned} \tag{3.16}$$

and there is also a contribution from the contour at infinity which has been set to zero by assuming that the frequency ω has a small negative imaginary part, which will eventually be made to tend to zero. The integral along $\mathcal{C}_- \cup \mathcal{C}_+$ can be replaced by a single integral along $\mathcal{C}$, with the integrand being replaced by the *jump* in the original integrand across $\mathcal{C}$ in the direction normal to the curve. Thus we have

$$I_i = \int_{\mathcal{C}} \left[G\frac{\partial}{\partial n}(\nabla^2 w_i) - w_i \frac{\partial}{\partial n}(\nabla^2 G) - (\nabla^2 w_i)\frac{\partial G}{\partial n} + (\nabla^2 G)\frac{\partial w_i}{\partial n} \right] \mathrm{d}s \tag{3.17}$$

and it is to be understood that the jumps apply only to w_i and its derivatives since G and its derivatives are continuous.

We now substitute the edge conditions satisfied by w_i on the curve $\mathcal{C}$ implied by (3.7) using the definitions of (2.9) and (2.10) to give

$$I_i = \int_{\mathcal{C}} \left[(\nabla^2 G)\frac{\partial w_i}{\partial n} - w_i \frac{\partial}{\partial n}(\nabla^2 G) \right] \mathrm{d}s + J_i^{(1)} + J_i^{(2)} \tag{3.18}$$

where

$$J_i^{(1)} = -\nu_1 \int_{\mathcal{C}} \left[G\frac{\partial}{\partial s}\left(\frac{\partial^2}{\partial s \partial n} - \theta'(s)\frac{\partial}{\partial s} \right) w_i \right] \mathrm{d}s \tag{3.19}$$

$$J_i^{(2)} = -\nu_1 \int_{\mathcal{C}} \left[\frac{\partial G}{\partial n}\left(\frac{\partial^2}{\partial s^2} + \theta'(s)\frac{\partial}{\partial n} \right) w_i \right] \mathrm{d}s. \tag{3.20}$$

Integrating by parts twice, in equation (3.19) first, gives

$$\begin{aligned} J_i^{(1)} = -\nu_1 \left[G\left(\frac{\partial^2}{\partial s \partial n} - \theta'(s)\frac{\partial}{\partial s} \right) w_i \right]\Big|_{-L}^{L} + \nu_1 \left[\frac{\partial G}{\partial s}\frac{\partial w_i}{\partial n} - \theta'(s)\frac{\partial G}{\partial s} w_i \right]\Big|_{-L}^{L} \\ -\nu_1 \int_{\mathcal{C}} \left[\frac{\partial^2 G}{\partial s^2}\frac{\partial w_i}{\partial n} - \frac{\partial}{\partial s}\left(\theta'(s)\frac{\partial G}{\partial s} \right) w_i \right] \mathrm{d}s. \end{aligned} \tag{3.21}$$

On account of the conditions (2.22) and (2.23) it is seen that the first and seconds term in the above equation vanish.

This leaves

$$J_i^{(1)} = -\nu_1 \int_{\mathcal{C}} \left[\frac{\partial^2 G}{\partial s^2}\frac{\partial w_i}{\partial n} - \frac{\partial}{\partial s}\left(\theta'(s)\frac{\partial G}{\partial s} \right) w_i \right] \mathrm{d}s. \tag{3.22}$$

Next, we consider $J_i^{(2)}$ in (3.20) and integrate by parts twice to obtain

$$J_i^{(2)} = -\nu_1 \left[\frac{\partial G}{\partial n}\frac{\partial w_i}{\partial s} \right]\Big|_{-L}^{L} + \nu_1 \left[\frac{\partial^2 G}{\partial s \partial n} w_i \right]\Big|_{-L}^{L} - \nu_1 \int_{\mathcal{C}} \left[\frac{\partial^3 G}{\partial s^2 \partial n} w_i + \theta'(s)\frac{\partial G}{\partial n}\frac{\partial w_i}{\partial n} \right] \mathrm{d}s \tag{3.23}$$

and again (2.22) can be used to show the first two terms vanish so that

$$J_i^{(2)} = -\nu_1 \int_{\mathcal{C}} \left[\frac{\partial^3 G}{\partial s^2 \partial n} w_i + \theta'(s)\frac{\partial G}{\partial n}\frac{\partial w_i}{\partial n} \right] \mathrm{d}s. \tag{3.24}$$

Using (3.22) and (3.24) in (3.18) and collecting together terms proportional to w_i and $\partial w_i/\partial n$ gives

$$\begin{aligned} I_i &= \int_{\mathcal{C}} \left[\big(\mathcal{B}G\big)(\boldsymbol{\rho};\alpha,\beta)\frac{\partial w_i}{\partial n} - w_i \big(\mathcal{S}G\big)(\boldsymbol{\rho};\alpha,\beta) \right] \mathrm{d}s \\ &= \int_{\mathcal{C}} \left\{ \big(\mathcal{B}G\big)(\boldsymbol{\rho};\alpha,\beta) \left[\frac{\partial w_i}{\partial n} \right] - \big(\mathcal{S}G\big)(\boldsymbol{\rho};\alpha,\beta)\big[w_i\big] \right\} \mathrm{d}s \end{aligned} \tag{3.25}$$

And now with $i = 1, 2$ separately and using (3.5), (3.6) we have

$$I_1 = \big(\mathcal{B}G\big)(\boldsymbol{\rho}; \alpha, \beta)|_{\boldsymbol{\rho}=\boldsymbol{\rho}_0}, \qquad I_2 = -\big(\mathcal{S}G\big)(\boldsymbol{\rho}; \alpha, \beta)|_{\boldsymbol{\rho}=\boldsymbol{\rho}_0}. \tag{3.26}$$

Using these expression in (3.12) with (3.11) to determine $A_i(\alpha, \beta)$ we readily obtain

$$\overline{\psi}_1 = -D\frac{\cosh k(z+h)}{K(k)}\big(\mathcal{B}G\big)(\boldsymbol{\rho}; \alpha, \beta)|_{\boldsymbol{\rho}=\boldsymbol{\rho}_0} \tag{3.27}$$

and

$$\overline{\psi}_2 = D\frac{\cosh k(z+h)}{K(k)}\big(\mathcal{S}G\big)(\boldsymbol{\rho}; \alpha, \beta)|_{\boldsymbol{\rho}=\boldsymbol{\rho}_0}. \tag{3.28}$$

Hence, if the function Ψ is defined by

$$\Psi(\boldsymbol{r}; \boldsymbol{\rho}_0) = \frac{1}{4\pi^2}\int_{-\infty}^{\infty}\int_{-\infty}^{\infty}\frac{\cosh k(z+h)}{K(k)}\mathrm{e}^{\mathrm{i}\alpha(x_0-x)}\mathrm{e}^{\mathrm{i}\beta(y_0-y)}\mathrm{d}\alpha\mathrm{d}\beta. \tag{3.29}$$

It then follows, from taking inverse transforms of (3.27) and (3.28) that

$$\psi_1(\boldsymbol{r}; \boldsymbol{\rho}_0) = -D\big(\mathcal{B}_0\Psi\big), \qquad \psi_2(\boldsymbol{r}; \boldsymbol{\rho}_0) = D\big(\mathcal{S}_0\Psi\big) \tag{3.30}$$

where $\mathcal{B}_0$ and $\mathcal{S}_0$ denote the same operators as in (2.9) and (2.10), but with (n_0, s_0) replacing (n, s). That is, these operators act on the source variables as opposed to the field variables.

3.4 The Green function for the sheet and its properties

A series expansion for the function Ψ is derived in the Appendix and is given by

$$\Psi(\boldsymbol{r}; \boldsymbol{\rho}_0) = \frac{\mathrm{i}}{4}\sum_{r=-2}^{\infty}\frac{Y_r(z)Y_r'(0)}{C_r}H_0(k_rR) \tag{3.31}$$

where $R = |\boldsymbol{\rho} - \boldsymbol{\rho}_0| = ((x-x_0)^2 + (y-y_0)^2)^{1/2}$. All other terms in (3.31) are defined in §2.3. The function Ψ is no more than the Green function for the time-harmonic point forcing of unit strength of the ice sheet at $\boldsymbol{\rho}_0$. Associated with Ψ is the corresponding ice sheet elevation, defined by

$$W(\boldsymbol{\rho}; \boldsymbol{\rho}_0) = \left.\frac{\partial\Psi}{\partial z}\right|_{z=0} = \frac{\mathrm{i}}{4}\sum_{r=-2}^{\infty}\tau_r H_0(k_rR) \tag{3.32}$$

where

$$\tau_r = \frac{(Y_r'(0))^2}{C_r}. \tag{3.33}$$

On first inspection, W appears to possess a logarithmic singularity as $R \to 0$, inherited from the behaviour of the Hankel function of the first kind, $H_0(k_rR) \equiv H_0^{(1)}(k_rR)$. However, this turns out not to be the case as we shall demonstrate. Using (3.30) in (3.13) in conjunction with (3.31) and (3.32) above shows that

$$w_1(\boldsymbol{\rho}; \boldsymbol{\rho}_0) = -D\big(\mathcal{B}_0W\big), \qquad w_2(\boldsymbol{\rho}; \boldsymbol{\rho}_0) = D\big(\mathcal{S}_0W\big). \tag{3.34}$$

The asymptotic expansion for $H_0(k_rR)$ is (see Abramowitz & Stegun (1965), for example)

$$H_0(z) = M_0 + \frac{2i}{\pi}\log z - \frac{iz^2}{2\pi}\log z + M_1z^2 + M_2z^4\log z + M_3z^4 + \ldots, \qquad z \to 0. \tag{3.35}$$

for certain coefficients $M_0, \ldots, M_3$ which we do not need to specify. Using this in combination with the relations

$$\sum_{r=-2}^{\infty} \tau_r = \sum_{r=-2}^{\infty} \tau_r k_r^4 = 0, \qquad \text{and} \qquad \sum_{r=-2}^{\infty} \tau_r k_r^2 = 1/D, \tag{3.36}$$

which were proved in the Appendix of Porter & Evans (2003) shows that

$$W(\boldsymbol{\rho}; \boldsymbol{\rho}_0) \sim M_4 + \frac{R^2 \log R}{8\pi D} + M_5 R^2 + M_6 R^4, \qquad R \to 0 \tag{3.37}$$

in terms of coefficients M_4, M_5, M_6 which again do not need to be specified. Thus, the elevation of the sheet due to a source of point forcing is bounded at the point of the forcing (as $R \to 0$) since there are no terms proportional to $\log R$. We also note that there is no term proportional to $R^4 \log R$ in the expression for W.

With this in mind, we write

$$W(\boldsymbol{\rho}; \boldsymbol{\rho}_0) = \widehat{W}(\boldsymbol{\rho}; \boldsymbol{\rho}_0) + \frac{R^2 \log R}{8\pi D} \tag{3.38}$$

where

$$\widehat{W}(\boldsymbol{\rho}; \boldsymbol{\rho}_0) = \frac{\mathrm{i}}{4} \sum_{r=-2}^{\infty} \tau_r \left(H_0(k_r R) - \frac{2\mathrm{i}}{\pi} \log R + \frac{i k_r^2}{2\pi} R^2 \log R \right) \tag{3.39}$$

now has at least six bounded derivatives as $R \to 0$.

3.5 Integral equations for the unknown functions P and Q

It remains for us to apply the two conditions at the edges of the crack and this will allow us to determine $P(s_0)$ and $Q(s_0)$ and hence the solution everywhere from (3.8). Thus, a careful application (explained in detail below) of (2.9) to (3.9) gives

$$-\frac{1}{8\pi} \mathcal{B} \left(\int_{\mathcal{C}} P(s_0) \mathcal{B}_0(R^2 \log R) \mathrm{d}s_0 \right) + \int_{\mathcal{C}} \left\{ P(s_0) \big(\mathcal{B}\widehat{w}_1\big)(\boldsymbol{\rho}; \boldsymbol{\rho}_0) + Q(s_0) \big(\mathcal{B} w_2\big)(\boldsymbol{\rho}; \boldsymbol{\rho}_0) \right\} \mathrm{d}s_0 = -\big(\mathcal{B}\eta_0\big)(\boldsymbol{\rho}) \tag{3.40}$$

and then (2.10) to (3.9) gives

$$\frac{1}{8\pi} \mathcal{S} \left(\int_{\mathcal{C}} Q(s_0) \mathcal{S}_0(R^2 \log R) \mathrm{d}s_0 \right) + \int_{\mathcal{C}} \left\{ P(s_0) \big(\mathcal{S} w_1\big)(\boldsymbol{\rho}; \boldsymbol{\rho}_0) + Q(s_0) \big(\mathcal{S}\widehat{w}_2\big)(\boldsymbol{\rho}; \boldsymbol{\rho}_0) \right\} \mathrm{d}s_0 = -\big(\mathcal{S}\eta_0\big)(\boldsymbol{\rho}) \tag{3.41}$$

both (3.40) and (3.41) holding for $\boldsymbol{\rho} \in \mathcal{C}$. The hatted functions $\widehat{w}_1$ and $\widehat{w}_2$ indicate that $\widehat{W}$ defined in (3.39) replaces W in the definitions (3.34).

In the derivation of the integral equations above, we have been careful to note that the compounded application of second and third-order boundary operators $\{\mathcal{B}, \mathcal{S}\}$, $\{\mathcal{B}_0, \mathcal{S}_0\}$ to the most singular part of the function W (namely $R^2 \log R/(8\pi D)$ where $R^2 = (x - x_0)^2 + (y - y_0)^2$) is potentially singular. Thus it can be confirmed that $\mathcal{B}(\mathcal{B}_0(R^2 \log R))$ is of order

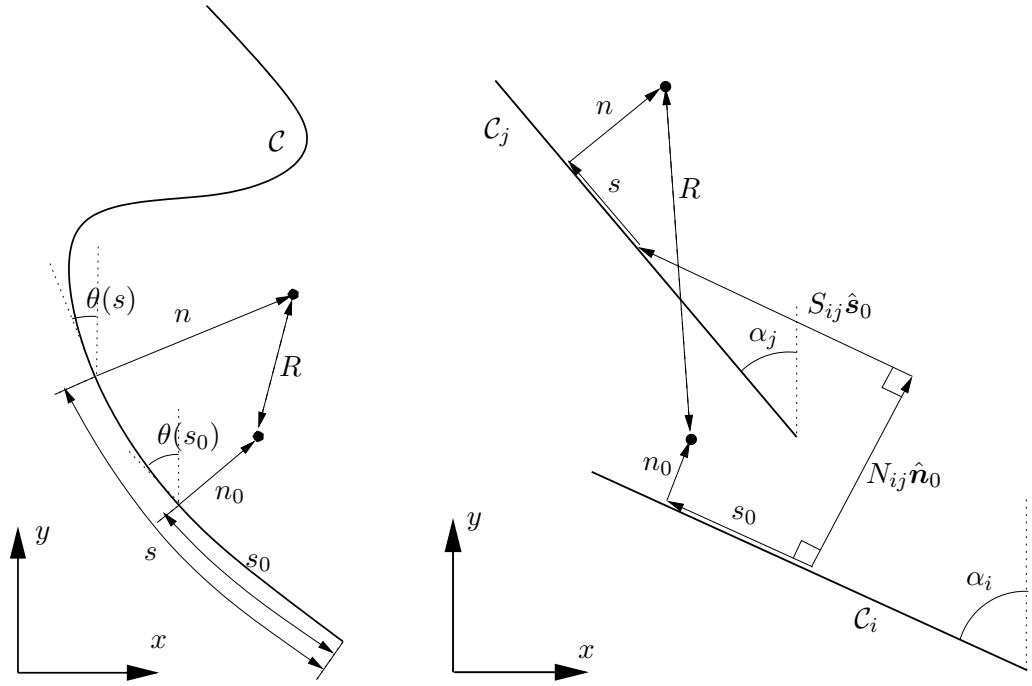

Figure 2: Definition of local coordinates on a single crack with curvature and two straight-line cracks.

R^{-2} and $\mathcal{S}(\mathcal{S}_0(R^2\log R))$ is of order R^{-4}, as $R\to 0$ and so the order of differentiation and integration cannot be interchanged (in the conventional sense) in the first terms of (3.40) and (3.41), as they have been for the second terms in each equation. It is possible to formulate hypersingular integral equations in which the differential operator is taken inside the integral, provided the integral is defined appropriately as a Hadamard finite part integral. For a detailed discussion of singular integral operators see Martin (2006, chapter 5).

Although the terms $\mathcal{B}(\mathcal{S}_0(R^2\log R))$ and $\mathcal{S}(\mathcal{B}_0(R^2\log R))$ also appear to be singular and of order R^{-3}, in fact they can be shown to be bounded as $R\to 0$ if, as has been assumed, $\mathcal{C}$ is a smooth curve. Thus, using the expression (3.42) below, it can be shown that $\partial R/\partial n = \partial R/\partial n_0 = 0$ whilst $\partial(\log R)/\partial n = -\partial(\log R)/\partial n_0 = \frac{1}{2}\theta'(s_0)$ for points on $\mathcal{C}$ as $R\to 0$.

The principal difficulty now is in applying boundary operators to functions of R. An alternative expression for R for a curve $\mathcal{C}$ with curvature $\theta'(s)$, is

$$R = \Bigg(\bigg(-\int_{s_0}^{s} \sin\theta(\xi)\mathrm{d}\xi + n\cos\theta(s) - n_0\cos\theta(s_0) \bigg)^2 + \bigg(\int_{s_0}^{s} \cos\theta(\xi)\mathrm{d}\xi + n\sin\theta(s) - n_0\sin\theta(s_0) \bigg)^2 \Bigg)^{1/2} \tag{3.42}$$

being the relative distance between points (n,s) and (n_0,s_0), n and n_0 measuring the distance away from, in a direction normal to, $\mathcal{C}$ at distances s and s_0 (respectively) along $\mathcal{C}$. This expression for R, is (arguably) the most useful if one wishes to apply the different operators $\mathcal{B}_0$, $\mathcal{S}_0$ etc. to the components of the Green function which require that derivatives are taken in s, s_0, n and n_0 (noting both n and n_0 are ultimately set to zero, when R represents the distance between two points on $\mathcal{C}$ itself).

An obvious simplification occurs if we take $\theta'(s) = 0$. Indeed, attempting to work with $\theta'(s) \neq 0$ appears to be frighteningly difficult, at least if one wishes to avoid resorting to fully numerical methods to solve (3.40) and (3.41).

Henceforth we shall consider cracks which are straight, at some fixed angle $\theta(s) = \alpha$ (measured anti-clockwise from the positive y-direction). This simplifies matters considerably and nearly every result below takes advantage of $\theta'(s) = 0$. Then (3.42) reduces to

$$R = \{((n-n_0)\cos\alpha - (s-s_0)\sin\alpha)^2 + ((n-n_0)\sin\alpha + (s-s_0)\cos\alpha)^2\}^{1/2}.$$

Also, $\mathcal{B} = \mathcal{B}_0$, $\mathcal{S} = -\mathcal{S}_0$ whilst it can be shown (after some algebra) that

$$\nabla^2(R^2\log R) = 4 + 4\log R, \qquad \frac{\partial^2}{\partial s^2}(R^2\log R) = (1 + 2\log R + 2R_s^2)$$

where $R_s \equiv \partial R/\partial s$. On $\mathcal{C}$ when $n = n_0 = 0$, $R = |s - s_0|$ and $R_s = \mathrm{sgn}(s - s_0)$. Thus we find that

$$-\frac{1}{8\pi}(\mathcal{B}(\mathcal{B}_0(R^2\log R))) = -\frac{1}{8\pi}\left(-2\nu_1\frac{\partial^2}{\partial s^2}\nabla^2 + \nu_1^2\frac{\partial^4}{\partial s^4}\right)(R^2\log R) = \frac{\sigma}{\pi}\frac{\partial^2}{\partial s^2}\log|s-s_0|$$

where $\sigma = \frac{1}{4}(1-\nu)(3+\nu)$ is the same as the quantity defined in Porter & Evans (2006b). We also find (using $\partial^2(\log R)/\partial n^2 = -\partial^2(\log R)/\partial s^2$) that

$$\frac{1}{8\pi}(\mathcal{S}(\mathcal{S}_0(R^2\log R))) = \frac{\sigma}{\pi}\frac{\partial^4}{\partial s^4}\log|s-s_0|.$$

Another important relation, which results from choosing $\theta'(s) = 0$ is that $\partial R/\partial n = -\partial R/\partial n_0 = 0$ for $n = n_0$ and for all $s, s_0 \in (-L, L)$ and this implies that $\big(\mathcal{B}w_2\big)(\boldsymbol{\rho};\boldsymbol{\rho}_0) = \big(\mathcal{S}w_1\big)(\boldsymbol{\rho};\boldsymbol{\rho}_0) = 0$ for $\boldsymbol{\rho}, \boldsymbol{\rho}_0 \in \mathcal{C}$.

Bringing everything together under our simplifying assumption of $\theta'(s) = 0$ allows (3.40) and (3.41) to be written

$$\frac{\sigma}{\pi}\frac{d^2}{ds^2}\int_{\mathcal{C}} P(s_0)\log|s-s_0|\mathrm{d}s_0 + \int_{\mathcal{C}} P(s_0)\big(\mathcal{B}\widehat{w}_1\big)(\boldsymbol{\rho};\boldsymbol{\rho}_0)\mathrm{d}s_0 = -\big(\mathcal{B}\eta_0\big)(\boldsymbol{\rho}) \tag{3.43}$$

and

$$\frac{\sigma}{\pi}\frac{d^4}{ds^4}\int_{\mathcal{C}} Q(s_0)\log|s-s_0|\mathrm{d}s_0 + \int_{\mathcal{C}} Q(s_0)\big(\mathcal{S}\widehat{w}_2\big)(\boldsymbol{\rho};\boldsymbol{\rho}_0)\mathrm{d}s_0 = -\big(\mathcal{S}\eta_0\big)(\boldsymbol{\rho}) \tag{3.44}$$

for $\boldsymbol{\rho} = (x(s), y(s)) \in C$.

3.6 Multiple cracks

A single straight-line crack and multiple parallel straight-line cracks have already been considered in the paper of Porter & Evans (2006b). Thus, in order that we use this method in a novel way, we shall consider the case of N distinct straight-line cracks which are orientated at arbitrary angles (and are of arbitrary length). This requires a slight modification to the formulation for the single crack previously presented.

In the case of N cracks, labelled $\mathcal{C}_i$, $i = 1, 2, \ldots, N$, the integral representation of the solution is found by superposition

$$\phi(\boldsymbol{r}) = \phi_0(\boldsymbol{r}) + \sum_{i=1}^{N} \int_{\mathcal{C}_i} \big\{ P_i(s_0)\psi_1(\boldsymbol{r};\boldsymbol{\rho}_0) + Q_i(s_0)\psi_2(\boldsymbol{r};\boldsymbol{\rho}_0) \big\} \mathrm{d}s_0 \tag{3.45}$$

with corresponding surface elevation

$$\eta(\boldsymbol{\rho}) = \eta_0(\boldsymbol{\rho}) + \sum_{i=1}^{N} \int_{\mathcal{C}_i} \big\{ P_i(s_0)w_1(\boldsymbol{\rho};\boldsymbol{\rho}_0) + Q_i(s_0)w_2(\boldsymbol{\rho};\boldsymbol{\rho}_0) \big\} \mathrm{d}s_0. \tag{3.46}$$

Now the $2N$ functions $P_i(s_0)$ and $Q_i(s_0)$, $i = 1, 2, \ldots, N$ represent the jumps in gradient and elevation across each of the N cracks.

Application of the boundary conditions at each of the cracks gives $2N$ coupled integral equations for the $2N$ unknowns,

$$\begin{aligned} &\frac{\sigma}{\pi}\frac{d^2}{ds^2}\int_{\mathcal{C}_j} P_j(s_0)\log|s-s_0|\mathrm{d}s_0 + \int_{\mathcal{C}_j} P_j(s_0)\big(\mathcal{B}\widehat{w}_1\big)(\boldsymbol{\rho};\boldsymbol{\rho}_0)\mathrm{d}s_0 \\ &\qquad \sum_{\substack{i=1\\ \neq j}}^{N} \int_{\mathcal{C}_i} \big\{ P_i(s_0)\big(\mathcal{B}w_1\big)(\boldsymbol{\rho};\boldsymbol{\rho}_0) + Q_i(s_0)\big(\mathcal{B}w_2\big)(\boldsymbol{\rho};\boldsymbol{\rho}_0) \big\} \mathrm{d}s_0 = -\big(\mathcal{B}\eta_0\big)(\boldsymbol{\rho}) \end{aligned} \tag{3.47}$$

and

$$\begin{aligned} &\frac{\sigma}{\pi}\frac{d^4}{ds^4}\int_{\mathcal{C}_j} Q_j(s_0)\log|s-s_0|\mathrm{d}s_0 + \int_{\mathcal{C}_j} Q_j(s_0)\big(\mathcal{S}\widehat{w}_2\big)(\boldsymbol{\rho};\boldsymbol{\rho}_0)\mathrm{d}s_0 \\ &\qquad \sum_{\substack{i=1\\ \neq j}}^{N} \int_{\mathcal{C}_i} \big\{ P_i(s_0)\big(\mathcal{S}w_1\big)(\boldsymbol{\rho};\boldsymbol{\rho}_0) + Q_i(s_0)\big(\mathcal{S}w_2\big)(\boldsymbol{\rho};\boldsymbol{\rho}_0) \big\} \mathrm{d}s_0 = -\big(\mathcal{S}\eta_0\big)(\boldsymbol{\rho}) \end{aligned} \tag{3.48}$$

for $\boldsymbol{\rho} \in \mathcal{C}_j$, $j = 1, \ldots, N$.

4 Reduction of the integral equations to an algebraic system of equations

The principal difficulty, already alluded to earlier, is in applying the boundary operators $\mathcal{B}_0$, $\mathcal{S}_0$ etc... to the Green function, W. This is still the case even after having made the simplifying assumption that each crack is straight.

The function W is a sum over Hankel functions of argument kR (here $k \equiv k_r$ for brevity). We find the integral representation of the Hankel function useful in what follows,

$$H_0(kR) = \frac{1}{i\pi}\int_{-\infty}^{\infty} \frac{\mathrm{e}^{\mathrm{i}lY}\mathrm{e}^{-\lambda|X|}}{\lambda(k,l)}\mathrm{d}l \tag{4.1}$$

where $\lambda(k,l) = (l^2-k^2)^{1/2} = -\mathrm{i}(k^2-l^2)^{1/2}$ and $R = |\boldsymbol{\rho}-\boldsymbol{\rho}_0|$, where $\boldsymbol{\rho} = (x,y)$, $\boldsymbol{\rho}_0 = (x_0,y_0)$ and $X = x - x_0$, $Y = y - y_0$. To be consistent with earlier work in this paper and to keep

the notation as simple as possible, variables with subscript zero will be associated with the crack $\mathcal{C}_i$ and those without with crack $\mathcal{C}_j$. We write the vector $\boldsymbol{\rho}-\boldsymbol{\rho}_0$ in terms of coordinates (n_0, s_0) local to $\mathcal{C}_i$

$$\boldsymbol{\rho}-\boldsymbol{\rho}_0 = X\hat{\boldsymbol{n}}_0 + Y\hat{\boldsymbol{s}}_0$$

where $\hat{\boldsymbol{n}}_0$ and $\hat{\boldsymbol{s}}_0$ are unit vectors aligned with the positive n_0 and s_0 directions, and the previous definitions of X and Y have been replaced with

$$\left.\begin{aligned} X &= N_{ij} - n_0 + s\sin A_{ij} + n\cos A_{ij} \\ Y &= S_{ij} - s_0 + s\cos A_{ij} - n\sin A_{ij} \end{aligned}\right\}, \qquad A_{ij} = \alpha_i - \alpha_j \tag{4.2}$$

where $N_{ij}\hat{\boldsymbol{n}}_0 + S_{ij}\hat{\boldsymbol{s}}_0$ is the vector from the centre of crack $\mathcal{C}_i$ (at an angle α_i) to crack $\mathcal{C}_j$ (at an angle α_j) in terms of coordinates local to crack $\mathcal{C}_i$. Angles of the cracks are measured counterclockwise from the positive y direction – see figure 2. Then

$$(\mathcal{B}(\mathcal{B}_0(H_0(kR)))) = \frac{1}{i\pi}\int_{-\infty}^{\infty} f_{11}(k,l,A_{ij})\frac{\mathrm{e}^{\mathrm{i}l(S_{ij}-s_0+s\cos A_{ij})}\mathrm{e}^{-\lambda|N_{ij}+s\sin A_{ij}|}}{\lambda}\mathrm{d}l \tag{4.3}$$

where

$$f_{11}(k,l,A) = (k^2-\nu_1 l^2)(k^2-\nu_1(l\cos A \pm \mathrm{i}\lambda\sin A)^2). \tag{4.4}$$

Henceforth the upper/lower signs indicate that the quantity $N_{ij}+s\sin A_{ij}$ is positive/negative for all $s\in[-L_j, L_j]$ (in other words $\pm$ can be replaced with $\mathrm{sgn}(N_{ij})$ and $\mp$ by $-\mathrm{sgn}(N_{ij})$). This imposes a geometric restriction, that the extension of any one crack cannot intersect any other crack. Note that only once the appropriate operators have been applied, are n and n_0 set to zero so that $\boldsymbol{\rho}_0\in\mathcal{C}_i$ and $\boldsymbol{\rho}\in\mathcal{C}_j$. Note also that if $\alpha_i=\alpha_j$ (either because s and s_0 are identified with the same crack, or because cracks are parallel) then $f_{11}(k,l,0)=(k^2-\nu_1 l^2)^2$.

We also have corresponding expressions for the compound operators $\mathcal{B}(\mathcal{S}_0)$, $\mathcal{S}(\mathcal{B}_0)$, $\mathcal{S}(\mathcal{S}_0)$ acting on $H_0(kR)$ with the functions f_{12}, f_{21} and f_{22} (respectively) taking the place of f_{11} in (4.3). Then we find

$$f_{12}(k,l,A) = \pm\lambda(k^2-\nu_1(l\cos A \pm \mathrm{i}\lambda\sin A)^2)(k^2+\nu_1 l^2) \tag{4.5}$$

$$f_{21}(k,l,A) = -\mathrm{i}(l\sin A \mp \mathrm{i}\lambda\cos A)(k^2-\nu_1 l^2)(k^2+\nu_1(l\cos A \pm \mathrm{i}\lambda\sin A)^2) \tag{4.6}$$

and

$$f_{22}(k,l,A) = \mp\mathrm{i}\lambda(l\sin A \mp \mathrm{i}\lambda\cos A)(k^2+\nu_1 l^2)(k^2+\nu_1(l\cos A \pm \mathrm{i}\lambda\sin A)^2). \tag{4.7}$$

As before, considerable simplification occurs if $\alpha_i=\alpha_j$.

Next, the unknown functions are expanded in an appropriate set of basis functions. According to (2.22) $P_i(s)/(L_i^2-s^2)^{1/2}$ and $Q_i(s)/(L_i^2-s^2)^{3/2}$, are bounded for all $s\in[-L_i, L_i]$ and can therefore be expanded in a complete set in $\mathrm{L}_2[-L_i, L_i]$. Thus we write

$$P_i(s_0) = \frac{(L_i^2-s_0^2)^{1/2}}{L_i^3}\sum_{n=0}^{\infty} a_n^{(i)}\frac{\mathrm{e}^{\mathrm{i}n\pi/2}}{(n+1)}U_n(s_0/L_i), \qquad s_0\in(-L_i, L_i) \tag{4.8}$$

and

$$Q_i(s_0) = \frac{2(L_i^2-s_0^2)^{3/2}}{L_i^4}\sum_{n=0}^{\infty} b_n^{(i)}\frac{\mathrm{e}^{\mathrm{i}n\pi/2}}{(n+1)(n+2)(n+3)}C_n^{(2)}(s_0/L_i), \qquad s_0\in(-L_i, L_i) \tag{4.9}$$

where the coefficients $a_n^{(i)}$, $b_n^{(i)}$, for $i = 1, 2, \ldots, N$ are to be determined and U_n, $C_n^{(2)}$ are the Chebychev polynomial of the second kind and the ultraspherical Gegenbauer polynomial, respectively. The extra normalising factors are included in (4.8) and (4.9) for later algebraic convenience and also to ensure that $a_n^{(i)}$ and $b_n^{(i)}$ are dimensionless (according to the definition of η, the dimensions of P_i and Q_i are inverse length squared and inverse length respectively).

The particular choice of orthogonal polynomials are made because of their association with the weighting functions in (4.8) and (4.9). In particular, they satisfy the orthogonality relationships

$$\int_{-L_i}^{L_i} (L_i^2 - s_0^2)^{1/2} U_n(s_0/L_i) U_m(s_0/L_i) \mathrm{d}s_0 = \tfrac{1}{2}\pi L_i^2 \delta_{mn}; \tag{4.10}$$

$$\int_{-L_i}^{L_i} (L_i^2 - s_0^2)^{3/2} C_n^{(2)}(s_0/L_i) C_m^{(2)}(s_0/L_i) \mathrm{d}s_0 = \tfrac{1}{8}\pi L_i^4 (m+3)(m+1)\delta_{mn}. \tag{4.11}$$

Expansions similar to (4.8), (4.9) were used by Porter & Evans (2006b) following Andronov & Belinksii (1995) who noted that the functions U_n and $C_n^{(2)}$ may be regarded as the eigenfunctions of the singular parts of the integral equations in the sense that they satisfy

$$\frac{d^2}{ds^2} \int_{-L_i}^{L_i} \ln|s - s_0| (L_i^2 - s_0^2)^{1/2} U_n(s_0/L_i) \mathrm{d}s_0 = \pi(n+1) U_n(s/L_i) \tag{4.12}$$

and

$$-\frac{d^4}{ds^4} \int_{-L_i}^{L_i} \ln|s - s_0| (L_i^2 - s_0^2)^{3/2} C_n^{(2)}(s_0/L_i) \mathrm{d}s_0 = \pi(n+3)(n+2)(n+1) C_n^{(2)}(s/L_i) \tag{4.13}$$

for $s \in (-L_i, L_i)$. These are crucial results which allow the hypersingular integrals (as Martin (2006) calls them) to be evaluated explicitly.

Also needed in making the required calculations that follow are the results

$$\int_{-L_i}^{L_i} \mathrm{e}^{\mathrm{i}us_0} (L_i^2 - s_0^2)^{1/2} U_n(s_0/L_i) \mathrm{d}s_0 = \frac{\mathrm{e}^{\mathrm{i}n\pi/2}(n+1)\pi L_i^2}{L_i u} J_{n+1}(L_i u) \tag{4.14}$$

and

$$\int_{-L_i}^{L_i} \mathrm{e}^{\mathrm{i}us_0} (L_i^2 - s_0^2)^{3/2} C_n^{(2)}(s_0/L_i) \mathrm{d}s_0 = \frac{\mathrm{e}^{\mathrm{i}n\pi/2}(n+3)(n+2)(n+1)\pi L_i^4}{2(L_i u)^2} J_{n+2}(L_i u) \tag{4.15}$$

(see for example, Gradshteyn & Ryzhik (1981)) where J_n is the Bessel function.

Finally, it can be shown, starting with the integral representation of the logarithm,

$$\log|x| = \frac{1}{2} \int_{-\infty}^{\infty} \frac{\mathrm{e}^{-|t|} - \mathrm{e}^{\mathrm{i}tx}}{|t|} \mathrm{d}t$$

that

$$\frac{d^2}{ds^2} \int_{-L}^{L} u(s_0) \log|s - s_0| \mathrm{d}s_0 = \frac{1}{2} \int_{-\infty}^{\infty} |l| \int_{-L}^{L} u(s_0) \mathrm{e}^{\mathrm{i}l(s-s_0)} \mathrm{d}s_0 \mathrm{d}l \tag{4.16}$$

and

$$-\frac{d^4}{ds^4} \int_{-L}^{L} u(s_0) \log|s - s_0| \mathrm{d}s_0 = \frac{1}{2} \int_{-\infty}^{\infty} l^2 |l| \int_{-L}^{L} u(s_0) \mathrm{e}^{\mathrm{i}l(s-s_0)} \mathrm{d}s_0 \mathrm{d}l \tag{4.17}$$

for suitable functions u such that the integrals exist.

Using these results, we can implement the following procedure – the details of the calculation are lengthy, but tedious and will therefore be omitted. Thus, we first substitute the expansions (4.8) and (4.9) into (3.47) and (3.48). The definitions of w_1, w_2 and their hatted versions defined by (3.34) with W, $\widehat{W}$ defined by (3.32) and (3.39) are simultaneously inserted into (3.47) and (3.48), where the representations (4.3) to (4.7) are used. The equation representing what was originally (3.47) is multiplied by the function $U_m(s/L_j)$ and what started out as (3.48) is multiplied by $C_m^{(2)}(s/L_j)$ and both are integrated between $-L_j$ and L_j. The various results (4.10)–(4.17) quoted above allow all the integrals over the cracks to be performed analytically.

The procedure outlined above is actually nothing more than the Rayleigh-Ritz/Galerkin method to the integral equations in which the residual is made orthogonal to the space spanned by $P_i(s)$ and $Q_i(s)$. If, as is here, the set of functions used in the expansion of $P_i(s)$ and $Q_i(s)$ are complete in the appropriate space, then the residual must be zero and the integral equations for unknowns P_i and Q_i have been replaced with an infinite algebraic system of equations for unknown expansion coefficients $a_n^{(i)}$ and $b_n^{(i)}$. Numerically, the infinite system of equations is truncated and the solution of the finite system is then only an approximation to the solution of the integral equations.

The system of equations that result from this process is written

$$\frac{\sigma}{(m+1)}a_m^{(j)} + \sum_{n=0}^{\infty} a_n^{(j)} K_{jjmn}^{(11)} + \sum_{\substack{i=1\\ \neq j}}^{N}\sum_{n=0}^{\infty}\left\{a_n^{(i)} K_{ijmn}^{(11)} + b_n^{(i)} K_{ijmn}^{(12)}\right\} = G_{jm}^{(1)} \tag{4.18}$$

and

$$-\frac{\sigma}{(m+2)}b_m^{(j)} + \sum_{n=0}^{\infty} b_n^{(j)} K_{jjmn}^{(22)} + \sum_{\substack{i=1\\ \neq j}}^{N}\sum_{n=0}^{\infty}\left\{a_n^{(i)} K_{ijmn}^{(21)} + b_n^{(i)} K_{ijmn}^{(22)}\right\} = G_{jm}^{(2)}. \tag{4.19}$$

It will take some time to define all the coefficients occurring in the above two equations. First

$$K_{ijmn}^{(11)} = -\frac{DL_j^3}{2L_i}\int_{-\infty}^{\infty}\sum_{r=-2}^{\infty}\tau_r \frac{f_{11}(k_r,l,A_{ij})}{\lambda(k_r,l)}\exp\{\mathrm{i}lS_{ij} - \lambda(k_r,l)|N_{ij}|)\} \times \frac{J_{n+1}(L_i l)J_{m+1}(L_j(l\cos A_{ij} \pm \mathrm{i}\lambda(k_r,l)\sin A_{ij}))}{(L_i l)(L_j(l\cos A_{ij} \pm \mathrm{i}\lambda(k_r,l)\sin A_{ij}))}\mathrm{d}l.$$

If $i = j$, then $A_{jj} = 0$ and $N_{jj} = S_{jj} = 0$ so that

$$K_{jjmn}^{(11)} = L_j^2\int_{-\infty}^{\infty}\left\{\frac{-D}{2}\sum_{r=-2}^{\infty}\tau_r\left(\frac{f_{11}(k_r,l,0)}{\lambda(k_r,l)} - \nu_1^2 l^2|l|\right) - \sigma|l|\right\}\frac{J_{n+1}(L_j l)J_{m+1}(L_j l)}{(L_j l)(L_j l)}\mathrm{d}l \tag{4.20}$$

in which terms included within the brackets are $O(1/|l|^3)$ and the integrand decays like $1/l^6$ as $|l| \to \infty$. The addition of the term $\sigma|l|$ is responsible for this decay and is derived from the term $R^2\log R$ which is included in the definition of $\widehat{W}$. The term $\nu_1^2 l^2|l|$ has zero net contribution to the sum, on account of the relation (3.33). Its appearance is as a direct

result of the term proportional to the $\log R$ term in the definition of $\widehat{W}$ and makes the decay of the series explicit.

From Gradshteyn & Ryzhik (1981, §6.538) we have

$$\int_{-\infty}^{\infty} \frac{J_n(L_j l)J_m(L_j l)}{|l|}\mathrm{d}l = \frac{\delta_{mn}}{m}, \qquad m = 1, 2, \ldots \tag{4.21}$$

which can be used to confirm that the first term in (4.18) is cancelled by the $\sigma|l|$ term in (4.20) and is an alternative view on the addition and subtraction of the $R^2 \log R$ term in the definition of $\widehat{W}$.

Next, we have

$$K_{ijmn}^{(12)} = \frac{DL_j^3}{2}\int_{-\infty}^{\infty}\sum_{r=-2}^{\infty}\tau_r \frac{f_{12}(k_r, l, A_{ij})}{\lambda(k_r, l)}\exp\{\mathrm{i}lS_{ij} - \lambda(k_r, l)|N_{ij}|\} \times \frac{J_{n+2}(L_i l)J_{m+1}(L_j(l\cos A_{ij} \pm \mathrm{i}\lambda(k_r, l)\sin A_{ij}))}{(L_i l)^2(L_j(l\cos A_{ij} \pm \mathrm{i}\lambda(k_r, l)\sin A_{ij}))}\mathrm{d}l.$$

Then,

$$K_{ijmn}^{(21)} = -\frac{DL_j^4}{2L_i}\int_{-\infty}^{\infty}\sum_{r=-2}^{\infty}\tau_r \frac{f_{21}(k_r, l, A_{ij})}{\lambda(k_r, l)}\exp\{\mathrm{i}lS_{ij} - \lambda(k_r, l)|N_{ij}|\} \times \frac{J_{n+1}(L_i l)J_{m+2}(L_j(l\cos A_{ij} \pm \mathrm{i}\lambda(k_r, l)\sin A_{ij}))}{(L_i l)(L_j(l\cos A_{ij} \pm \mathrm{i}\lambda(k_r, l)\sin A_{ij}))^2}\mathrm{d}l$$

and

$$K_{ijmn}^{(22)} = \frac{DL_j^4}{2}\int_{-\infty}^{\infty}\sum_{r=-2}^{\infty}\tau_r \frac{f_{22}(k_r, l, A_{ij})}{\lambda(k_r, l)}\exp\{\mathrm{i}lS_{ij} - \lambda(k_r, l)|N_{ij}|\} \times \frac{J_{n+2}(L_i l)J_{m+2}(L_j(l\cos A_{ij} \pm \mathrm{i}\lambda(k_r, l)\sin A_{ij}))}{(L_i l)^2(L_j(l\cos A_{ij} \pm \mathrm{i}\lambda(k_r, l)\sin A_{ij}))^2}\mathrm{d}l.$$

For $i = j$ in the last equation, we get

$$K_{jjmn}^{(22)} = L_j^4\int_{-\infty}^{\infty}\left\{\frac{D}{2}\sum_{r=-2}^{\infty}\tau_r\left(\frac{f_{22}(k_r, l, 0)}{\lambda(k_r, l)} - \nu_1^2 l^4|l|\right) + \sigma l^2|l|\right\}\frac{J_{n+2}(L_j l)J_{m+2}(L_j l)}{(L_j l)^2(L_j l)^2}\mathrm{d}l \tag{4.22}$$

where again the presence of the term $\sigma l^2|l|$ is on account of the $R^2 \log R$ term and (4.21) can be used to show that its contribution directly cancels the first term of (4.19). The integrand in (4.22) decays like $1/l^6$ as $|l| \to \infty$.

Finally, the right-hand side terms in (4.18), (4.19) which are derived from the forcing from the incident wave are given by

$$G_{jm}^{(1)} = 2k_0^2 L_j^3(1 - \nu_1\sin^2(\varphi - \alpha_j))Y_0'(0) \times \exp\{ik_0(x_j\cos\varphi + y_j\sin\varphi)\}\frac{J_{m+1}(k_0 L_j\sin(\varphi - \alpha_j))}{k_0 L_j\sin(\varphi - \alpha_j)} \tag{4.23}$$

and

$$G_{jm}^{(2)} = 2\mathrm{i}k_0^3 L_j^4(1 + \nu_1\sin^2(\varphi - \alpha_j))\cos(\varphi - \alpha_j)Y_0'(0) \times \exp\{ik_0(x_j\cos\varphi + y_j\sin\varphi)\}\frac{J_{m+2}(k_0 L_j\sin(\varphi - \alpha_j))}{(k_0 L_j\sin(\varphi - \alpha_j))^2} \tag{4.24}$$

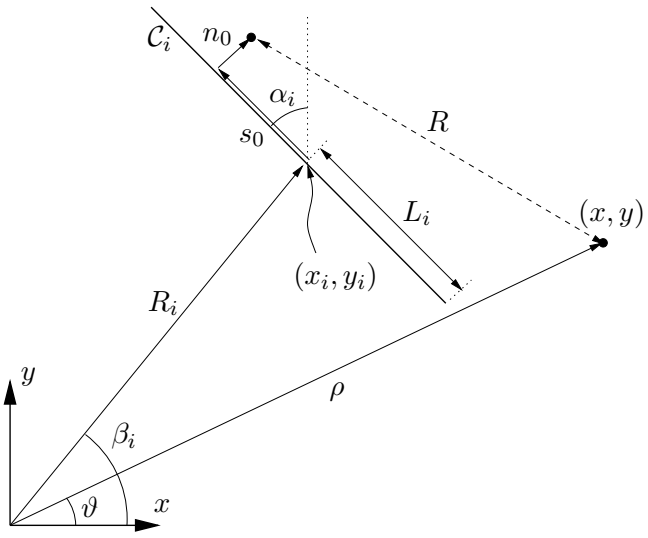

Figure 3: Geometrical description of the position of a crack relative to the origin.

where the centre of the jth crack, angled at α_j to the positive y-axis and of length L_j, is at (x_j, y_j) with respect to the fixed Cartesian origin. As a reminder, φ is the angle of the incident wave measured from the positive x-axis.

All the elements of the coupled systems of equations in (4.8), (4.9) are dimensionless, and it should be noted that the integration variable l has dimensions of a wavenumber.

The system of equation coincides exactly with that of Porter & Evans (2006b) in the case where $\alpha_i = 0$ for all $i = 1, \ldots, N$.

5 Properties of the solution

5.1 Plate elevation and far field diffracted waves

Here, we are interested in the behaviour of the diffracted wave elevations on the elastic plate, given by

$$\lim_{\rho\to\infty} \phi_d(\boldsymbol{r}) = \lim_{\rho\to\infty} (\phi(\boldsymbol{r}) - \phi_0(\boldsymbol{r})) = \sqrt{\frac{2\pi}{k\rho}}\mathcal{A}(\vartheta;\varphi)\mathrm{e}^{\mathrm{i}(k\rho-\pi/4)}Y_0(z) \tag{5.1}$$

where $\rho = |\boldsymbol{\rho}| = \sqrt{x^2+y^2}$, $(x, y) = \rho(\cos\vartheta, \sin\vartheta)$. Here, $\mathcal{A}(\vartheta;\varphi)$ is the diffraction coefficient (or directivity) measuring the circular wave amplitude in the direction ϑ due to an incident wave travelling at an angle φ. Of course, $\eta_d = \partial\phi_d/\partial z|_{z=0}$.

We use the integral representation given by (3.8) assuming that the functions P_i and Q_i are given by (4.8), (4.9) and the coefficients have been found from solving the linear system of equations (4.18) and (4.19). First, we align coordinate axes with the ith crack, so that the relative vector $X\hat{\boldsymbol{n}}_0 + Y\hat{\boldsymbol{s}}_0$ between two points, one based on the crack itself is

$$X = \rho\cos(\vartheta-\alpha_i) - R_i\cos(\beta_i-\alpha_i) - n_0, \qquad Y = \rho\sin(\vartheta-\alpha_i) - R_i\sin(\beta_i-\alpha_i) - s_0$$

where $(x_i, y_i) = R_i(\cos\beta_i, \sin\beta_i)$ are the polar coordinates to the centre of the ith crack, angled α_i to the positive y-direction. The variable $s_0 \in (-L_i, L_i)$ measures the distance

along that crack, n_0 will eventually be set to zero once the differential operators have been applied. This is used in (4.1) so that

$$(\mathcal{B}_0 H_0(kR)) = \frac{1}{\pi \mathrm{i}} \int_{-\infty}^{\infty} \frac{g_1(k,l)}{\lambda} \exp\{\mathrm{i}\rho(l\sin(\vartheta-\alpha_i) \pm \mathrm{i}\lambda\cos(\vartheta-\alpha_i))\} \\ \times \exp\{-\mathrm{i}R_i(l\sin(\beta_i-\alpha_i) \pm \mathrm{i}\lambda\cos(\beta_i-\alpha_i))\}\mathrm{e}^{-\mathrm{i}ls_0}\mathrm{d}l$$

where

$$g_1(k,l) = -(k^2 - \nu_1 l^2)$$

and, as before the upper/lower signs correspond to the sign of the quantity $\rho\cos(\vartheta-\alpha_i) - R_i\cos(\beta_i-\alpha_i)$, which measures if the field point is to the 'right' or 'left' (in terms of the local coordinates) of the ith crack.

The corresponding expression for $(\mathcal{S}_0 H_0(kR))$ is as above, but with g_1 replaced by

$$g_2(k,l) = \mp\lambda(k^2 + \nu_1 l^2).$$

After some algebra, we find that

$$\phi_d = \frac{D}{4}\sum_{i=1}^{N}\left\{\sum_{n=0}^{\infty} a_n^{(i)} U_n^{(i)}(\rho,\vartheta,z) + \sum_{n=0}^{\infty} b_n^{(i)} V_n^{(i)}(\rho,\vartheta,z)\right\} \tag{5.2}$$

where

$$U_n^{(i)}(\rho,\vartheta,z) = -\frac{1}{L_i}\sum_{r=-2}^{\infty}\frac{Y_r'(0)Y_r(z)}{C_r}\int_{-\infty}^{\infty}\frac{g_1(k_r,l)}{\lambda(k_r,l)}\exp\{\mathrm{i}\rho(l\sin(\vartheta-\alpha_i) \pm \mathrm{i}\lambda(k_r,l)\cos(\vartheta-\alpha_i))\} \\ \times\exp\{-\mathrm{i}R_i(l\sin(\beta_i-\alpha_i) \pm \mathrm{i}\lambda(k_r,l)\cos(\beta_i-\alpha_i))\}\frac{J_{n+1}(L_i l)}{L_i l}\mathrm{d}l$$

and

$$V_n^{(i)}(\rho,\vartheta,z) = \sum_{r=-2}^{\infty}\frac{Y_r'(0)Y_r(z)}{C_r}\int_{-\infty}^{\infty}\frac{g_2(k_r,l)}{\lambda(k_r,l)}\exp\{\mathrm{i}\rho(l\sin(\vartheta-\alpha_i) \pm \mathrm{i}\lambda(k_r,l)\cos(\vartheta-\alpha_i))\} \\ \times\exp\{-\mathrm{i}R_i(l\sin(\beta_i-\alpha_i) \pm \mathrm{i}\lambda(k_r,l)\cos(\beta_i-\alpha_i))\}\frac{J_{n+2}(L_i l)}{(L_i l)^2}\mathrm{d}l.$$

The expressions above can be used to define the elevation of the elastic plate throughout the entire (x,y) domain. In order to determine the far field wave amplitudes, we make a change of integration variable, writing $l = k_0\sin w$ and hence $\lambda(k_0,l) = -\mathrm{i}k_0\cos w$. The contour of integration in the complex w-plane is chosen to lie along the three line segments $\{-\frac{1}{2}\pi + \mathrm{i}\infty < w < -\frac{1}{2}\pi\} \cup \{-\frac{1}{2}\pi < w < \frac{1}{2}\pi\} \cup \{\frac{1}{2}\pi < w < \frac{1}{2}\pi - \mathrm{i}\infty\}$. Then,

$$U_n^{(i)}(\rho,\vartheta,z) \sim -\frac{\mathrm{i}Y_0'(0)Y_0(z)}{L_i C_0}\int g_1(k_0,k_0\sin w)\exp\{\pm\mathrm{i}k_0\rho\cos(\vartheta-\alpha_i\mp w)\} \\ \times\exp\{\mp\mathrm{i}k_0 R_i\cos(\beta_i-\alpha_i\mp w)\}\frac{J_{n+1}(k_0 L_i\sin w)}{k_0 L_i\sin w}\mathrm{d}w$$

where we have anticipated the fact that the $r=0$ propagating mode will have the dominant effect in the far field. The dominant contribution from the integral, in the limit as $\rho\to\infty$

is given by the saddle point method, which finds the stationary point to be at $w = \vartheta - \alpha_i$ for $-\frac{1}{2}\pi < \vartheta - \alpha_i < \frac{1}{2}\pi$ and $w = \pi - \vartheta + \alpha_i$ for $\frac{1}{2}\pi < \vartheta - \alpha_i < \frac{3}{2}\pi$. Then,

$$U_n^{(i)}(\rho,\vartheta,z) \sim \sqrt{\frac{2\pi}{k_0\rho}}\mathrm{e}^{\mathrm{i}(k_0\rho-\pi/4)}\left\{\frac{-\mathrm{i}Y_0'(0)Y_0(z)}{L_iC_0}g_1(k_0,k_0\sin(\vartheta-\alpha_i),\alpha_i)\right.$$
$$\left.\times\exp\{-\mathrm{i}k_0R_i\cos(\beta_i-\vartheta)\}\frac{J_{n+1}(k_0L_i\sin(\vartheta-\alpha_i))}{k_0L_i\sin(\vartheta-\alpha_i)}\right\} \quad (5.3)$$

Similarly, we find

$$V_n^{(i)}(\rho,\vartheta,z) \sim \sqrt{\frac{2\pi}{k_0\rho}}\mathrm{e}^{\mathrm{i}(k_0\rho-\pi/4)}\left\{\mp\frac{Y_0'(0)Y_0(z)}{C_0}g_2(k_0,k_0\sin(\vartheta-\alpha_i),\alpha_i)\right.$$
$$\left.\times\exp\{-\mathrm{i}k_0R_i\cos(\beta_i-\vartheta)\}\frac{J_{n+2}(k_0L_i\sin(\vartheta-\alpha_i))}{(k_0L_i\sin(\vartheta-\alpha_i))^2}\right\} \quad (5.4)$$

These expressions are bounded at $\vartheta = \alpha_i$, a fact which follows from the behaviour of the Bessel functions for small argument.

It follows from using (5.3) and (5.4) in (5.2) with (5.1) that

$$\mathcal{A} = \frac{DY_0'(0)}{4C_0}\sum_{i=1}^{N}\mathrm{e}^{-ik_0R_i\cos(\beta_i-\vartheta)}\sum_{n=0}^{\infty}\left\{\frac{a_n^{(i)}}{L_i}g_1(k_0,k_0\sin(\vartheta-\alpha_i))\frac{J_{n+1}(k_0L_i\sin(\vartheta-\alpha_i))}{k_0L_i\sin(\vartheta-\alpha_i)}\right.$$
$$\left.\mp b_n^{(i)}g_2(k_0,k_0\sin(\vartheta-\alpha_i))\frac{J_{n+2}(k_0L_i\sin(\vartheta-\alpha_i))}{(k_0L_i\sin(\vartheta-\alpha_i))^2}\right\}.$$

Finally, a comparison with (4.23) and (4.24) reveals that a much more compact expression for the diffracted wave field exists

$$\mathcal{A}(\vartheta;\varphi) = -\frac{D}{8C_0}\sum_{i=1}^{N}\sum_{n=0}^{\infty}\left\{\frac{a_n^{(i)}\left(G_{in}^{(1)}\right)^*}{L_i^4}+\frac{b_n^{(i)}\left(G_{in}^{(2)}\right)^*}{L_i^4}\right\}$$

where * denotes complex conjugation.

A check on the numerical procedure is provided by the conservation of energy relation (see Porter & Evans (2006b), for example),

$$\Sigma = \frac{1}{2\pi}\int_0^{2\pi}|\mathcal{A}(\vartheta;\varphi)|^2\mathrm{d}\vartheta = -\frac{1}{\pi}\Re\{\mathcal{A}(\varphi;\varphi)\} \quad (5.5)$$

where Σ is called the scattering cross-section. It is likely, (although it has not been proved) that this energy relation is satisfied automatically by any approximation (i.e. any truncation of the infinite system of the equations).

5.2 Stress intensity factors

At the ends of each of the cracks, an important quantity to consider is the stress intensity factor (SIF), a measure of the magnitude of the lateral stresses acting at the crack tip. According to linear elastic theory, the stresses are singular at the tip (in reality, no singularity

would exist and there would be a small region of plastic deformation at the tip), and so the SIF is defined to be a multiplicative factor associated with that singularity. Thus, we define,

$$K^{\pm} = \lim_{s \to \pm L_i^{\pm}} \sqrt{\pm 2\pi (s - L_i^{\pm})} \sigma_n(s)$$

in which the definition of s is extended outside the interval $[-L_i, L_i]$ so that the limit is taken approaching the ends of the cracks from within the elastic plate. The stress in a direction normal to the direction of the crack is given by

$$\sigma_n(s) = \frac{Ed}{2(1-\nu^2)} \left(\nu \frac{\partial^2 \eta}{\partial s^2} + \frac{\partial^2 \eta}{\partial n^2} \right)$$

evaluated at its maximum on the upper and lower surfaces of the plate. A prolonged calculation, the details of which can be found in Porter & Evans (2006b) for the case of parallel straight line cracks gives an identical result to Porter & Evans (2006b), namely

$$K_i^{\pm} = \mathrm{i} \sqrt{\frac{\pi}{L_i}} \frac{Ed(3+\nu)}{8(1+\nu)L_i^2} \sum_{n=0}^{\infty} a_n^{(i)} \mathrm{e}^{\pm \mathrm{i} n \pi/2}.$$

This is not surprising, since the SIF is dominated by the effects local to the crack itself, and so its orientation and proximity with respect to other cracks will not feature in this expression. It is also worthy of note that the SIF can be seen to be proportional to the rate of change of the jump in elevation along the crack. Thus, using the property, $U_n(\pm 1) = (n+1)(\pm 1)^n$, of the Chebychev polynomial shows that

$$P_i(s) \sim \frac{(L_i^2 - s^2)^{1/2}}{L_i^3} \sum_{n=0}^{\infty} a_n^{(i)} \mathrm{e}^{\pm \mathrm{i} n \pi/2}, \qquad \text{as } s \to -L_i^+, L_i^-.$$

6 Numerical procedure and results

The majority of the computational effort goes into the calculation of the infinite integrals $K_{ijmn}^{(11)}$ etc. The main aim has been to compute these integrals to an 8 decimal place accuracy using a simple 10-point Gaussian quadrature rule. When $i \neq j$, the integrals are very easy to compute since they have an exponential factor (which is exponential in both the integration variable l and the summation index r) to assist convergence. The rate of exponential decay is determined by the minimum distance between any two points on a crack, as projected normal to the crack (the value of $|N_{ij}| - L_j| \sin A_{ij}|$).

The most difficult integrals to compute are $K_{jjmn}^{(11)}$ and $K_{jjmn}^{(22)}$ whose convergence is not assisted by exponential decay, but nevertheless have integrands which decay like $1/l^6$. Thus, it was found that sufficient accuracy was obtained by truncating infinite integrals to the range $-2 < l < 2$ and choosing 10000 Guass points. The infinite series in r was truncated to a maximum of 2000, although this figure was only ever needed for $i = j$ when there was no assisted convergence from exponential decay.

The remaining parameter that ultimately determines the accuracy of the scheme is the level of truncation of the infinite system of equations (4.18) and (4.19). The choice of truncation size required for a desired level of accuracy depends upon the ratio of wavelength to the length of a crack. This is because the oscillations along the crack, which increase with

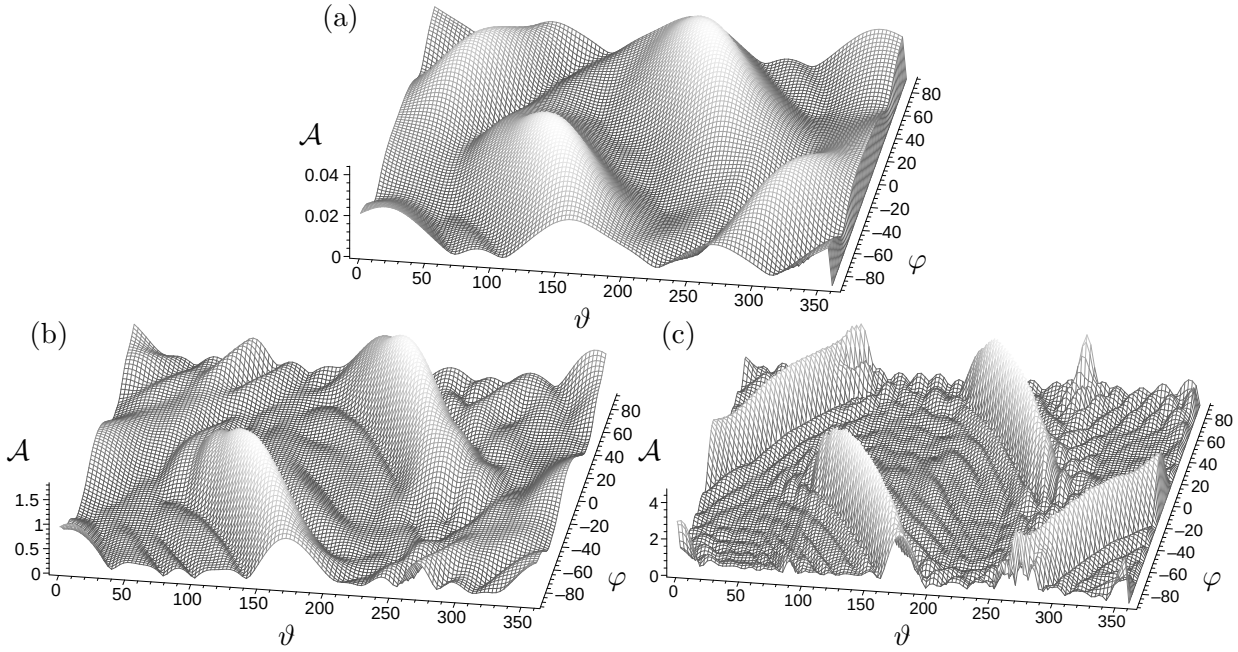

Figure 4: Diffraction coefficient $\mathcal{A}(\vartheta;\varphi)$ for two cracks in a right-angled V formation – see text for parameters: (a) $\lambda = 200$m; (b) $\lambda = 100$m; (c) $\lambda = 50$m.

the ratio of length of crack to wavelength, need a sufficient number of functions to model them accurately. Experimentation has shown that the truncation size should be determined by the value of the integer part of $\max_i\{k_0 L_i\}$. For example, a wavelength of 100m impinging on a series of cracks of maximum length 200m would require truncation to six terms in the series for five decimal place accuracy in the solution, whereas a wavelength of 200m would only require three terms for the same accuracy. Thus the truncated versions of equations (4.18) and (4.19) represent a relatively small system of equations which can be solved quite efficiently.

The energy relation (5.5) is used to check the results although it gives no indication of the accuracy of the method because the integral in (5.5) is approximated numerically (also see remarks made after (5.5). When there is only one crack, or there are multiple parallel cracks, we recover the results of Porter & Evans (2006b), although this is expected since the formulation of the system of equations is identical to that of Porter & Evans (2006b) in these cases. We shall therefore focus results on multiple, non-parallel crack configurations.

The physical parameters used are as follows (these are typical values used for sea ice). So $E = 5 \times 10^9$Pa, $\nu = 0.3$, $\rho_w = 1025$kgm-3, $\rho_i = 925.5$kgm^{-3}, $g = 9.81$ms^{-2} We shall perform all calculations with an ocean depth of $h = 40$m and for an ice thickness of $d = 1$m; results for larger depths are almost identical to results for this depth whilst the qualitative aspects are altered only very slightly with different values of d.

In figure 4 we show typical results for the diffraction coefficient $\mathcal{A}(\vartheta;\varphi)$ measuring the wave amplitude factor of outgoing waves in the direction ϑ due to an incident wave propagating at φ. The arrangement considered in figure 4 are for waves of wavelength (a) 200m, (b) 100m and (c) 50m impinging on two cracks with geometric parameters $(x_i,\, y_i,\, L_i,\, \alpha_i)$ of: $i = 1$ (-80m, 0m, 100m, 135°), $i = 2$ (80m, 0m, 100m, 45°). The cracks are thus of length 200m and are at 90° to one another, roughly forming a V. The symmetry of the configuration implies that we need only consider $-90° < \varphi < 90°$. What can be noticed is that there are

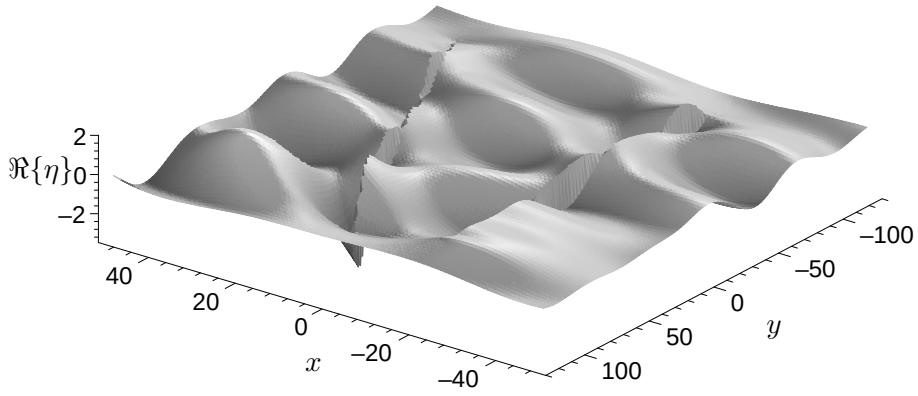

Figure 5: Snapshot of the ice sheet elevation for two cracks (x_i, y_i, L_i, α_i) of: $i = 1$ (-20m, 0m, 100m, 0°), $i = 2$ (20m, 0m, 100m, 10°) and $\varphi = 45°$, $\lambda = 50$m.

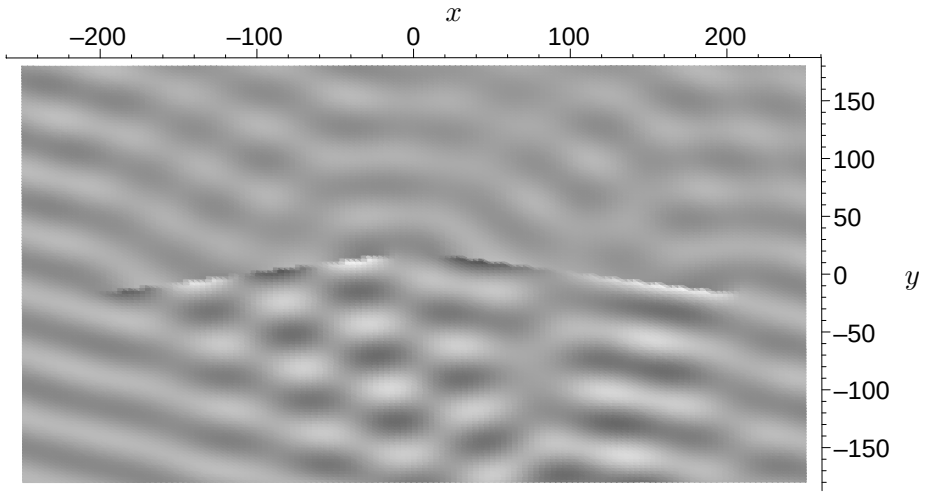

Figure 6: Plan view of a snapshot of the ice sheet elevation for two cracks (x_i, y_i, L_i, α_i) of: $i = 1$ (-110m, 0m, 100m, 100°), $i = 2$ (110m, 0m, 100m, 80°) and $\varphi = 70°$, $\lambda = 50$m. Light/dark shading represent peaks/troughs.

large peaks in the diffraction due to reflection (and to a lesser extent transmission) of the plane waves from the straight cracks, which become more pronounced as the wavelength decreases and little sign of interaction between the cracks resulting in any other significant peak in the diffraction coefficient.

In figure 5 we show a snapshot in time of the wave elevation on the ice sheet for two cracks angled at 10° to one another – see figure caption for details. The surface elevation data is generated on a Cartesian grid, which is awkward to resolve on cracks which are not aligned with the x or y axes. Convention dictates that the incident wave is set at unit amplitude. The largest amplitudes throughout a period of incident wave are found at the leeward edge of the left-hand crack, being approximately four.

A plan view of the wave field in the presence of two cracks of a different configuration is shown in figure 6. In this example, in which there is a small ($\approx$ 20m) gap between two slightly out-of-line cracks each of length 200m, the diffracted wave pattern can clearly be seen. There is substantial reflection from the two cracks, giving rise to quite large amplitudes (up to four)

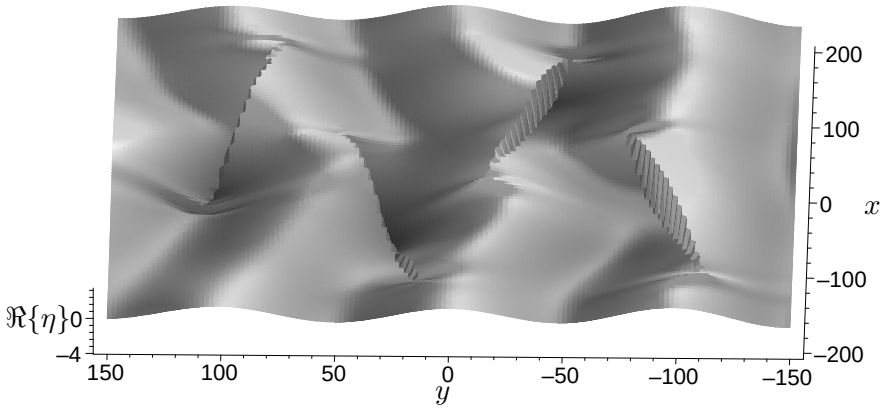

Figure 7: Snapshot of the ice sheet elevation for four cracks (x_i, y_i, L_i, α_i) of: $i = 1$ (-60m, -93m, 100m, 100°), $i = 2$ (60m, -31m, 100m, 80°), $i = 3$ (-60m, 31m, 100m, 100°), $i = 4$ (60m, 93m, 100m, 80°) and $\varphi = 90°$, $\lambda = 100$m.

along the front faces of the cracks. This is unsurprising since the reflection coefficient for an infinitely long straight-line crack at this wavelength is close to unity (see Evans & Porter (2003), for example). There is little response from the ice sheet in the small gap between the cracks although a circular wave front can be observed propagating outwards from the gap on the leeward side in addition to the circular waves transmitted from the outer edges of the two cracks.

Figure 7 provides another snapshot for an arrangement of four nearly parallel cracks under beam incidence. Again, the cracks are all 200m in length and the wavelength is chosen to be 100m. Here the response in elevation in the region around the cracks is quite large, being up to five times the incident wave height.

In the last two figures, **??**(a) and (b) stress intensity factors are presented as a function of wavenumber k_0 (2π/wavelength).

7 Conclusions

In this paper, we have considered the scattering of plane flexural gravity waves in ice sheets on water by narrow cracks of arbitrary shape. The main result has been to show that the solution of the problem may be expressed in terms of functions which are determined as the solution of a coupled system of integro-differential equations. Two key difficulties have been identified with the computation of numerical solutions to these equations the case of general-shaped cracks. The first is how to treat the component of the equations which contains the integro-differential operator and the second is how to compute the bounded parts of the kernels, which are defined to be complicated differential operators associated with the edge conditions on the cracks applied twice to a non-trivial Green function. It is possible that both difficulties may be overcome by using a fully numerical scheme to solve the integro-differential equations although this would appear to be non-trivial and has not been considered further in this paper. Instead, we have focused on multiple straight-line cracks of arbitrary orientation and have shown in this case that both difficulties can be overcome although the details are somewhat complicated. A key part of the success of the approach we have used is to expand the unknown functions in the space of functions which include

the correct behaviour at the end points of the cracks. We have also made use of an integral representation of the Green function and changes in coordinate systems to assist in the application of the fourth to sixth order differential operators. The system of equations that are derived and the numerical results we have computed match up with those independently computed for parallel straight-line cracks in Porter & Evans (2006b).

When the density of the fluid, ρ_w is set to zero, one the problem is reduced to that of flexural wave diffraction with cracks in a thin elastic sheet *in vacuo*. In this case, the dispersion relation is reduced to $k^4 = \rho_i d\omega^2/F$ where $F = Ed^3/(12(1-\nu^2))$ is the flexural rigidity of the sheet. The two independent roots are $k = (\rho_i d\omega^2/F)^{1/4}$ and $\mathrm{i}k$. The Green function, $W(\boldsymbol{\rho};\boldsymbol{\rho}_0)$, defined in (3.32) is replaced with

$$W = \frac{\mathrm{i}}{8k^2D}\left(H_0(kR) - H_0(\mathrm{i}kR)\right)$$

where $R = |\boldsymbol{\rho} - \boldsymbol{\rho}_0|$ (see Norris & Vermula (1995), eqn.(28)) which can be derived by taking Fourier transforms. As $R \to 0$, it can be shown that

$$W \sim \frac{\mathrm{i}}{8k^2D} + \frac{R^2 \log R}{8\pi D}.$$

That is, the Green function for the *in vacuo* case has the same properties as the Green function for the ice sheet but is very much reduced in complexity, being just the difference of two Hankel functions. It follows that the same methods used in this paper can be applied to the problem of an elastic plate *in vacuo*.

It is also anticipated that the methods introduced in this paper should be capable of being adpated for the simpler case of 'pinned' lines in elastic plates, either *in vacuo* or bounded by a fluid. Indeed, this problem will be somewhat simpler, as the second and third order boundary conditions $\mathcal{B}\eta = 0$ and $\mathcal{S}\eta = 0$ are replaced by $\eta = 0$ and $\partial\eta/\partial n = 0$. A further extension being considered involves cracks in elastic plates which contain sharp corners or kinks.

Appendix: The function Ψ

Consider a function $\Psi(\boldsymbol{r};\boldsymbol{\rho}_0)$ which satisfies

$$\Delta\Psi = 0, \qquad \boldsymbol{r} \in \mathcal{W}$$

with $\partial\Psi/\partial z = 0$ on $z = -h$ and

$$(\mathcal{L}\Psi)(\boldsymbol{\rho};\boldsymbol{\rho}_0) \equiv (D\nabla^4 + 1 - \delta)\Psi_z|_{z=0} - \kappa\Psi|_{z=0} = \delta(x - x_0)\delta(y - y_0).$$

This is a Green function for a time-harmonic forcing of unit strength of an ice sheet at a point $\boldsymbol{\rho}_0$. By taking transforms in x and y in the manner outlined at the beginning of §3, we readily find that

$$\Psi(\boldsymbol{r};\boldsymbol{\rho}_0) = \frac{1}{4\pi^2}\int_{-\infty}^{\infty}\int_{-\infty}^{\infty}\frac{\cosh k(z+h)}{K(k)}\mathrm{e}^{\mathrm{i}\alpha(x_0-x)}\mathrm{e}^{\mathrm{i}\beta(y_0-y)}\mathrm{d}\alpha\mathrm{d}\beta \tag{A.1}$$

where $k^2 = \alpha^2 + \beta^2$. This is the function introduced in the main part of the paper in (3.29) and $K(k)$ is defined in (2.15). It follows that

$$\Psi = \frac{1}{2\pi}\int_0^{\infty}\frac{\cosh k(z+h)}{K(k)}kJ_0(kR)\mathrm{d}k \tag{A.2}$$

where $R = |\boldsymbol{\rho} - \boldsymbol{\rho}_0|$ after making the substitutions $\alpha = k\cos w$, $\beta = k\sin w$, $x - x_0 = R\cos v$, $y - y_0 = R\sin v$ and and using the identity

$$J_0(kR) = \frac{1}{2\pi}\int_0^{2\pi} \mathrm{e}^{\mathrm{i}kR\cos w} dw. \tag{A.3}$$

Following Fox & Chung (1998), we define

$$f(\zeta) = \frac{\cosh\zeta(z+h)}{K(\zeta)} \tag{A.4}$$

where $f(\zeta)$ has poles at $\zeta = \pm k_r$, $r = -2, -1, 0, 1, \ldots$. Then consider the integral, for $\zeta \neq \pm k_r$,

$$\frac{1}{2\pi\mathrm{i}}\oint_C \frac{f(\zeta')}{\zeta' - \zeta}\mathrm{d}\zeta' = f(\zeta) + \sum_{r=-2}^{\infty}\left(\frac{\mathrm{Res}(f : k_r)}{k_r - \zeta} - \frac{\mathrm{Res}(f : -k_r)}{k_r + \zeta}\right) \tag{A.5}$$

where C is a circular contour whose radius tends to infinity and $\mathrm{Res}(f : k)$ denotes the residue of the function $f(\zeta)$ at $\zeta = k$. Setting $\zeta = 0$ in the above gives

$$\frac{1}{2\pi\mathrm{i}}\oint_C \frac{f(\zeta')}{\zeta'}\mathrm{d}\zeta' = f(0) + \sum_{r=-2}^{\infty}\left(\frac{\mathrm{Res}(f : k_r)}{k_r} - \frac{\mathrm{Res}(f : -k_r)}{k_r}\right). \tag{A.6}$$

Now

$$\frac{1}{2\pi\mathrm{i}}\oint_C \frac{f(\zeta')}{\zeta'}\mathrm{d}\zeta' = \frac{1}{2\pi\mathrm{i}}\oint_C \frac{\cosh\zeta'(z+h)}{\zeta' K(\zeta')}\mathrm{d}\zeta' = 0$$

since the integrand is $O(k^{-6})$ as $|k| \to \infty$. We can use the fact that $\mathrm{Res}(f : k_r) = \cosh k_r(z+h)/K'(k_r) = Y_r(z)/K'(k_r)$ where $K'(\zeta) = -K'(-\zeta)$ so show that $\mathrm{Res}(f : k_r) = -\mathrm{Res}(f : -k_r)$. This results in the identity

$$f(0) = -2\sum_{r=-2}^{\infty}\frac{\mathrm{Res}(f : k_r)}{k_r} \tag{A.7}$$

which translates to

$$\sum_{r=-2}^{\infty}\frac{Y_r(z)Y_r'(0)}{k_r^2 C_r} = 1$$

once $f(0) = -1$ and $K'(k_r) = 2k_r C_r/Y_r'(0)$, with C_r defined by (2.17) have been used. Subtracting (A.6) from (A.5) gives

$$\frac{\zeta}{2\pi\mathrm{i}}\oint_C \frac{f(\zeta')}{\zeta'(\zeta' - \zeta)}\mathrm{d}\zeta' = f(\zeta) + \sum_{r=-2}^{\infty}\frac{2k_r\mathrm{Res}(f : k_r)}{k_r^2 - \zeta^2}$$

and now it can be shown that the left-hand side vanishes (Fox & Chung (1998)) so that finally,

$$f(\zeta) = \sum_{r=-2}^{\infty}\frac{2k_r\mathrm{Res}(f : k_r)}{\zeta^2 - k_r^2}$$

Returning to the definition of f in (A.4) and substituting into (A.3) and (A.2) we have

$$\Psi = \frac{1}{\pi}\sum_{r=-2}^{\infty}\frac{k_r\cosh k_r(z+h)}{K'(k_r)}\int_0^{\infty}\frac{kJ_0(kR)}{k^2 - k_r^2}\mathrm{d}k$$

and the integral can be evaluated explicitly (see Abramovitz & Stegun (1965)) to $\frac{1}{2}\pi \mathrm{i} H_0(k_r R)$ where $H_0(x)$ denotes the Hankel function of the first kind to give

$$\Psi = \frac{\mathrm{i}}{4} \sum_{r=-2}^{\infty} \frac{Y_r(z) Y_r'(0)}{C_r} H_0(k_r R)$$

after substituting for $K'(k_r)$.

References

[1] Abramowitz, M.A. & Stegun, I. (eds), 1965. *Handbook of Mathematical Functions.* New York: Dover.

[2] Andronov, I.V. & Belinksii, B.P., 1995. Scattering of a flexural wave by a straight finite crack in an elastic plate. *J. Sound Vib.* **180**(1), 1–16.

[3] Balmforth, N.J. & Craster, R.V., 1999. Ocean waves and ice sheets. *J. Fluid Mech.* **395**, 89–124.

[4] Barrett, M.D. & Squire, V.A., 2002. Ice-coupled wave propagation across an abrupt change in ice rigidity, density or thickness. *J. Geophys. Res.* **101**(C9), 20825–20832.

[5] Evans, D.V. & Porter, R., 2003. Wave scattering by narrow cracks in ice sheets floating on water of finite depth. *J. Fluid Mech.* **484**, 143–165.

[6] Fox, C. & Chung, H., 1998. Green's function for forcing of a thin elastic plate. *Number 408, Department of Mathematics, Research Reports series, University of Auckland.*

[7] Gradshteyn, I.S. & Ryzhik, I.M., 1980. *Table of Integrals, Series and Products*, Fourth Edition. New York: Academic Press.

[8] Norris, A.N. & Vemula, C., 1995. Scattering of flexural waves on thin plates. *J. Sound Vib.* **181**(1), 115–125.

[9] Norris, A.N. & Wang, Z., 1994. Bending-wave diffraction from strips and cracks on thin plates. *Q. J. Mech. Appl. Math.,* **47**(4), 607–627.

[10] Martin, P.A., 2006. *Multiple Scattering. Interaction of Time Harmonic Waves with N Obstacles.* Cambridge: Cambridge University Press.

[11] Porter, R. & Evans, D.V., 2006*a*. Scattering or flexural waves by multiple narrow cracks in ice sheets floating. *Wave Motion,* **43**(5), 425–443.

[12] Porter, R. & Evans, D.V., 2006*b*. Diffraction of flexural waves by finite straight cracks in an elastic sheet over water. *J. Fluids & Struct.,* (In publication).

[13] Squire, V.A. & Dixon A.W., 2001. How a region of cracked sea ice affects ice-coupled wave propagation. *Annals Glaciol.,* **33**, 327–332.

[14] Squire, V.A., Dugan, J.P., Wadhams, P., Rottier, P.J., & Liu, A.K., 1995. Of ocean waves and ice sheets. *Ann. Rev. Fluid Mech.,* **27**, 115–168.

[15] Timoshenko, S. & Woinowsky-Krieger, S., 1959. *Theory of Plates and Shells*, Second Edition. New York: McGraw-Hill.

[16] Vaughan, G.L. & Squire, V.A., 2006. Scattering of ice-coupled waves by ice sheets by variable sea-ice terrain. *Annals Glaciol.,* **44**, 159–168.

[17] Williams, T., 2005. *Reflections on ice: Scattering of flexural-gravity waves by irregularities in Arctic and Antarctic ice sheets.* Ph.D. Thesis, University of Otago, Dunedin University, New Zealand.

[18] Williams, T.D. & Squire, V.A., 2002. Wave propagation across an oblique crack in an ince sheet. *Int. J. Offshore & Polar Engng.,* **12**(3), ???–???.

[19] Williams, T.D. & Squire, V.A., 2004. The scattering of flexural-gravity waves by an ice field. *Int. J. Offshore & Polar Engng.* **14**(3), 161–168.